Study on the Machinability of Natural Fiber-based Hybrid Composite with Nanofiller Incorporation

A thesis submitted in partial fulfillment of the requirements for the degree of

Master of Science in Mechanical Engineering

by

Md. Nayem Uddin

Student ID: 19MME015P

Department of Mechanical Engineering

Chittagong University of Engineering & Technology, Chattogram-4349

APPROVAL

The thesis titled "Study on the Machinability of Natural Fiber-based Hybrid Composite with Nanofiller Incorporation", submitted by Md. Nayem Uddin, Student ID: 19MME015P, Session: 2019-20, has been accepted as satisfactory in partial fulfillment of the requirements for the degree of Master of Science in Mechanical Engineering on September 2024.

BOARD OF EXAMINERS

………………………………………………………………… **Chairman**

Dr. Md. Sanaul Rabbi (Supervisor)

Professor, Dept. of Mechanical Engineering, CUET

………………………………………………………………… **Member**

Dr. Mohammad Mizanur Rahman (Ex-officio)

Professor & Head, Dept. of Mechanical Engineering, CUET

………………………………………………………………… **Member**

Dr. Sajal Chandra Banik

Professor, Dept. of Mechanical Engineering, CUET

………………………………………………………………… **Member**

Dr. Md. Mamunur Roshid

Professor, Dept. of Mechanical Engineering, CUET

………………………………………………………………… **Member**

Dr. Md. Mostaqur Rahman (External)

Professor, Dept. of Mechanical Engineering, DUET

DECLARATION

I, the undersigned, do hereby confirm to declare that the thesis is conducted and composed by myself and the work has not been submitted anywhere for other degrees or professional qualifications. To the best of my knowledge, contained materials were not written or published by anyone, except where due references are made.

Name: Md. Nayem Uddin

Student ID: 19MME015P

ACKNOWLEDGMENT

At first, the author wants to exhibit his gratitude to the almighty Allah for his boundless, spontaneous and continuous kindness in the successful completion of the thesis works.

Then the author would like to express his heartfelt acknowledgment and profound indebtedness to his thesis supervisor, Dr. Md. Sanaul Rabbi, Professor, Department of Mechanical Engineering, Chittagong University of Engineering and Technology, Chattogram-4349, under whose immeasurable and continuous supervision this thesis was carried out. His affectionate suggestions, valuable guidance and heartiest inspirations made this thesis finished throughout the work.

The author would like to exhibit his gratitude to the head, the faculty members, the officers and the staffs of the respective department, for their heartiest supports, suggestions, and help to use the laboratory facility in completing the thesis work.

The author wants to extend his acknowledgment to the head of the Department of Mechanical Engineering, Dhaka University of Engineering and Technology, Gazipur, for his permission to use the laboratory facility of his department.

The author wishes to express his special thanks to the members of the examination committee for their valuable suggestions and observations to enrich the thesis. Finally, the author would like to expand his heartfelt gratitude to his family members for their substantial supports and encouragement throughout the thesis work.

ABSTRACT

In many industrial applications, natural fiber reinforced composites are emerging as a competitive substitute of composites based on synthetic fibers due to their numerous advantages. However, real world applications of such composites require some secondary operations in order to complete the assembly of the components or parts. This work focuses on preparing hybrid composite made of glass and jute fiber along with epoxy composites incorporated with nanofiller and investigating the machinability of those composites. Hand lay-up technique was used to prepare the composites with five layers of fibers. Three types of nanoparticle such as Al_2O_3, ZnO, and TiO_2 of 3 wt.% were incorporated into the composites. Machinability was assessed considering the delamination factor and surface roughness. Analytical studies of machinability were conducted using minitab software. The findings show that the addition of nanofillers considerably increases the machining performance of the composite material. Comparing among three different nanofillers it was found that the composite contains the ZnO nanoparticle provided the significant improvement with least overall surface roughness and moderate delamination. On the contrary, TiO_2 incorporated composite material showed least delamination.

সার-সংক্ষেপ

অনেক শিল্প প্রতিষ্ঠানে, প্রাকৃতিক তন্তু দ্বারা সুসংগঠিত কম্পজিট সিনথেটিক ফাইবারের তুলনায় বহুবিধ সুবিধার কারনে একটি প্রতিযোগিতামূলক বিকল্প হিসেবে আবির্ভূত হচ্ছে । এই ধরনের কম্পজিটগুলোর বাস্তব বিশ্বের যথাযথ এপ্লিকেশনের জন্য সেকেন্ডারি অপারেশন প্রয়োজন । এই গবেষণাটির মূল প্রতিপাদ্য বিষয় হলো, গ্লাস ও পাটের আঁশের সমন্বয়ে ইপক্সি পলিমারের সংমিশ্রণে সহ কম্পজিট প্রস্তুত করা এবং সেগুলোর মেশিনাবিলিটি যাচাই-বাছাই করা । কম্পজিটগুলো প্রস্তুত করা হয়েছে হ্যান্ড লে-আপ কৌশল ব্যাবহার করে যেখানে ফাইবারগুলোর ক্রম পরিবর্তন করার মাধ্যমে স্যাম্পলে বৈচিত্র্যতা রক্ষা করা হয়েছে । নির্দিষ্ট অনুপাত বজায় রেখে মোট তিন ধরনের ন্যানো-পার্টিকেল স্যাম্পল তৈরিতে ব্যবহার করা হয়েছে যথা, এলুমিনিয়াম, জিঙ্ক এবং টাইটানিয়াম অক্সাইড । প্রতিটি স্যাম্পলের মেশিনাবিলিটি যাচাই করার জন্য ও পৃষ্ঠের রুক্ষতা নিরূপণ করা হয়েছে। বিশ্লেষণাত্মক অধ্যয়নের জন্য মিনিট্যাব সফটওয়্যার ব্যাবহার করা হয়েছে । ভিন্ন ভিন্ন ন্যানো-পার্টিকেল দ্বারা তৈরিকৃত স্যম্পলের মেশিনাবিলিটি নিরূপণ করে একটি তুলনামূলক অধ্যয়ন উপস্থাপন করা হয়েছে । তুলনায় দেখা যায়, জিঙ্ক-অক্সাইড সমৃদ্ধ স্যাম্পল ন্যূনতম পৃষ্ঠরুক্ষতা এবং টাইটানিয়াম অক্সাইড সমৃদ্ধ স্যাম্পল ন্যূনতম ডিলামিনেশন ফলাফল প্রদান করেছে ।

TABLE OF CONTENTS

LIST OF FIGURES

LIST OF TABLES

Chapter 1
Introduction

1.1 PREFACE

Composite materials composed of natural fibers and a matrix substance, like a polymer or a biodegradable substance, are known as natural fiber composites. Plant-based fibers like jute, flax, hemp, sisal, bamboo, and kenaf, as well as animal-based fibers like wool and silk, are frequently utilized in these composites. In recent years, these materials have drawn more attention as a sustainable substitute for conventional composite materials, which are frequently derived from non-renewable resources. Among the many benefits of natural fiber composites are their low cost, low density, high specific strength, and stiffness. They are renewable, biodegradable, and have good acoustic and thermal insulation qualities. Applications for natural fiber composites are numerous and include consumer items, packaging, building, and automobiles. Applications like the automotive sector, which demand a blend of low weight, high strength, and outstanding acoustic and thermal insulation qualities, are especially well-suited for them. Natural fiber composites have many benefits, but they can have drawbacks, such as inconsistent performance and variable fiber characteristics.

1.2 BACKGROUND

Natural fiber reinforcement is not a novel idea. Seventy years ago, people used natural fibers to meet their fundamental needs for clothes, food, and shelter [1]. Ancient civilizations like the Egyptians, who reinforced mud bricks with straw, are credited with developing natural fiber composites. In more recent times, With the creation of natural fiber reinforced polymers (NFRP) in the 1950s and 1960s, the use of natural fibers in composite materials got underway. But as a sustainable substitute for conventional composite materials, natural fiber composites did not receive much attention until the 1990s. Researchers are encouraged to investigate the possibilities of employing natural fibers in novel industries by the confluence of environmental regulations and industrial demands. Despite this, there is still a lack of research in this field, and numerous recent publications suggest that more study is necessary. [2].

Since NFC has a greater potential and is now being evaluated as a substitute for carbon or glass fiber composites, its research area has expanded. Among many other applicable industries, NFC is becoming more and more in demand, particularly in the automotive sector, because to its lightweight design and sound attenuation capability, which improves fuel efficiency. Furthermore, NFRPs can be designed to have advantageous qualities including acoustic and thermal insulation as well as a lower specific weight than their mineral-filled equivalents [3]. Jute and banana fibers are abundant in Bangladesh and Asia and are comparatively inexpensive to produce and manufacture when compared to other natural fibers. They belong to the high lignocellulose fiber category and have excellent mechanical qualities, which make them the perfect reinforcement for a variety of fibrous composites. The strong tensile and flexural strength of jute and banana fibers makes them ideal for composite construction. In Bangladesh, bananas and jute are also widely available. In addition to having beneficial qualities over conventional materials, synthetic fiber-reinforced Composites can be tailored to fulfill certain requirements. However, the synthetic fiber-reinforced composites are neither recyclable nor biodegradable in any form after their useful lives are finished. Environmental sensitivity concerns are being caused by these problems. Investigating workable options that might help with these issues is therefore essential. Natural fibers may be a viable substitute for synthetic fibers due to their many benefits, including low manufacturing costs, high stiffness, specific strength, environmental friendliness, and lack of toxicity. However, most composites based on natural fibers are not as strong as those constructed with synthetic fibers because the mechanical properties of natural fibers are significantly worse than those of synthetic fibers. Natural fiber composites also have low heat resistance, poor dimensional stability, unpredictability in characteristics, high susceptibility to moisture absorption, and incompatibility with polymeric matrices, leading to insufficient adhesion at the fiber/matrix interface. As a result, natural fiber in the polymer matrix alone cannot sufficiently meet all of the technical specifications for a fiber-reinforced composite.

A practical answer to these issues is the hybridization of synthetic and natural fiber within the same matrix. The best use of each fiber's properties can be achieved by combining natural and synthetic fibers in the same matrix material to produce an excellent but reasonably priced composite. To lessen the limits of each natural fiber, hybrid composites can also be successfully made using two different natural fibers. A hybrid composite material is defined by Sanchez [4] as a mixture of organic and inorganic materials with a micrometric level of mixing. However, a hybrid material is a combination of two or more materials whose size and shape have been adjusted to perform a certain purpose as effectively as feasible, according to Ashby [5]. The mechanical properties of composites are known to be considerably changed by the addition of fibers, either natural or synthetic, to a polymer.

Machinability is an important factor for giving the desired shape and size of the composite material which makes them usable for various applications. In many situations, NFRP composites must be machined in order to make the assembly of functioning components easier. Because bolts or rivets require holes to be machined, drilling is very important. It is well known that this machining process can cause a number of damage types in the machined composite components, including fiber pull-outs, delamination, and inter-laminar crack propagation, which can lead to hole-roundness problems [6]. The ability of jute fiber to strengthen polymer composites has been extensively studied and reported. Numerous characteristics, including fiber properties, fiber orientation, staple length, matrix properties, and fiber-matrix interface strength, are the main emphasis of FRP composites' attributes. The development of composites based on natural fibers has been viewed as a potential replacement for glass-fiber-based composites, particularly in numerous significant structural application industries such as the automotive, aerospace, and civil construction sectors. The manufacturing of car body panels, interiors, storage devices, building and industrial panels, etc., can be made more affordably with these composites-based items. [7] These days, automakers are encouraged to investigate renewable materials as alternatives to conventional materials while producing automobiles, particularly in light of the European Union's End of Life Vehicle (ELV) requirements. By adopting lightweight natural fiber reinforced plastic for the door panel and bumper, a vehicle's weight can be reduced and its fuel efficiency significantly boosted [8]. Primary and secondary manufacturing are two broad categories into which the manufacture of the NFRCs falls.

In actuality, NFRCs are primarily made utilizing a variety of primary composite fabrication techniques, including pultrusion, vacuum bag molding, resin transfer molding, and manual lay-up, which give the finished product a nearly net shape. To meet the requirements for part assembly, these near-net shapes still require certain secondary processes like drilling, milling, or turning. As a result, machining—particularly drilling—becomes essential to make part assembly easier [9]. To support the usage of natural fiber composites in certain use case scenarios, adequate research is required. The machinability of fiber reinforced polymer composites (FRPCs) has been the subject of numerous in-depth reviews, particularly edited publications. As most of the research is focused on fabrication and manufacturing of composites, research regarding machinability if jute fiber composite is limited and banana fiber composite is close to none. Very few research has been done on machinability of NFRCs. In context of Bangladesh, it is very important to examine the performance and machinability of NFRCs based on our own local fiber resources such as jute, banana, rattan. Coir, sisal etc. as our country has a huge potential to develop applications of NFRCs.

1.3 PROPERTIES OF NATURAL FIBRE BASED NANO COMPOSITES

The mechanical characteristics of hybrid polymer composites are influenced by multiple variables. The dispersion and distribution of reinforcements within the selected polymer matrix, interfacial adhesion between the polymer and reinforcements, big surface area, high aspect ratio, mechanical characteristics of reinforcements, loading effect, surface modification, fiber dimension, and orientation in the case of natural fibers are some of these factors. Many studies typically provide mechanical parameters as a function of size, loading, and fiber treatment [10] . Numerous factors affect the mechanical properties of hybrid polymer composites. Among these are the mechanical properties of reinforcements, loading effect, surface modification, fiber dimension, orientation in the case of natural fibers, interfacial adhesion between the polymer and reinforcements, large surface area, high aspect ratio, and the dispersion and distribution of reinforcements within the chosen polymer matrix. Mechanical parameters as a function of size, stress, and fiber treatment are commonly provided by numerous research [11]. The utilization of many reinforcing types is justified by the ability of one type's benefit to offset one type's drawback, hence enhancing the final material's performance and characteristics. While there are many benefits to using natural fibers, there are also some drawbacks. Even though they seem more appealing, they are not as strong, have a lower modulus, and have comparatively less moisture resistance than composites reinforced with synthetic fibers. Natural fibers' excessive moisture absorption is its primary drawback. This phenomenon weakens the interfacial bond between the fiber and the polymer matrix, leading to a decline in mechanical properties. Some fibers, such as lingo-cellulosic fiber, are too sensitive to moisture to be employed as reinforcement in composite materials because they generate even-dimensional instability. These characteristics limit natural fibers' ability to successfully reinforce polymer composites. Scientists are working harder to make use of these lignocellulosic fibers that occur naturally. The properties of lignocellulosic composites have been enhanced by a number of methods, such as chemical and physical pretreating of the fiber. In addition, hybridizing the lignocellulosic fibers with a more robust and corrosion-resistant synthetic fiber, such as glass fiber, can significantly improve the lignocellulosic composite's strength, stiffness, moisture resistance, and fire resistance. Table 1.1 displays some of the typical natural fibers' properties.

Table 1.1: Selected Physico-mechanical properties of some hybrid nano composites

Natural /synthetic Fiber	**Nano Filler**	**Matrix**	**Tensile strength (MPa)**	**Flexural Strength (MPa)**	**Ref.**
Glass/Silk	Ca_2SiO_4	Epoxy	0.0125	0.0016	
Jute/Glass	TiO_2	Polyester	62-77	121-182	[12]
Coir/Basalt	TiC	Epoxy	107.89	100	[13]
Jute-glass fiber	SiO_2	Epoxy	72.5	-	[14]
Kenaf/Glass	TiO_2(7.5%)	Epoxy	101	151	[15]

GFRP	Nano sisal	Polyurethane	18.7	26.8	[16]
Glass-Flax	MWCNT (1%)	Epoxy	432.5	0.00923	[17]
sisal-palm-glass fiber	SiO_2 (3%)	Epoxy	329.81	244.81	[18]
Sisal/ glass fiber	1wt% of MWCNT	Epoxy	234.5	56	[19]

1.4 OBJECTIVES

The objectives of this research are as stated below

(i) To prepare Jute, Banana, and Glass fiber reinforce composite with metal oxide nanofiller.

(ii) To conduct different machining operations on the prepared composite such as, milling and drilling operation.

(iii) To investigate the surface roughness and delamination factor after machining processes using Regression analysis.

(iv) To analyze the effect of spindle speed, cutting force, and feed rate on machining properties of the composite.

1.5 OUTLINE OF METHODOLOGY

The outline of the research work is presented below in Figure 1.1 as a flow chart

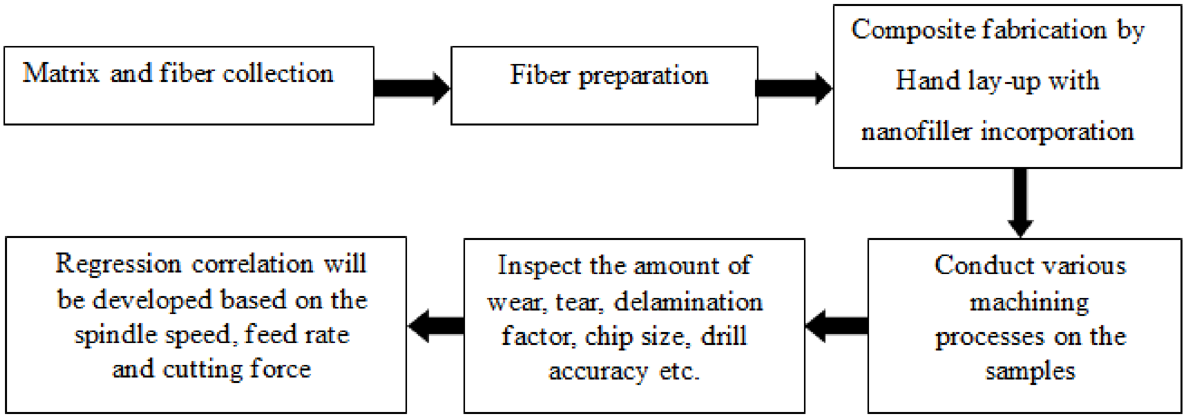

Figure 1.1: Outline of the methodology in flow chart.

1.6 SCOPES AND LIMITATIONS

Jute is well known worldwide for their fiber properties. They are extensively produced all over Bangladesh. Bangladesh is also famous for exporting jute all over the world. The application of jute fibers is mainly limited to ropes and bags as other possibilities are totally ignored. A proper study regarding their use as composite along with machining test can open new doors to a renewable future. Also, an increase of usage of natural fiber based composite materials as a replacement of plastic will also have a huge impact in reducing plastic waste which is a major concern for our country. A study on the machinability on the NFRCs fabricated from our own local natural resources can pave the way to future development of composites in our country. There is also scope of testing with different combination of fiber materials for various nanoparticle incorporation and achieve an ideal result through comparison.

The cost of producing composites and their functional characteristics determine whether NFRCs are used. They are utilized in consumer goods, packaging, the building and construction sector (ceiling panels, partition boards), transportation (automobiles, railroad coaches, and aircraft), and the military. When used as building materials, NFRCs are incredibly affordable for false partitions, ceilings, boards, walls, floors, window and door frames, roof tiles, and mobile or prefabricated buildings that can be utilized during natural disasters like earthquakes, floods, and cyclones. Without extensive machining during component assembly, applications would not be feasible. Therefore, machining is a crucial production step that requires comprehension, particularly when milling NFRCs. The way that NFRCs behave differs significantly from how traditional metallic materials are machined. Composite material machining necessitates a deeper comprehension of the cutting process in terms of precision and effectiveness. The impact of tool geometry and material on the damage to the hole resulting from composite anisotropy, which causes various types of damage, should be carefully considered. This research will pave the way to have a better understanding of how different nanofillers reacts with the matrix and fiber materials and also it will compare final machining performance of same composite used with aluminum, titanium and zinc oxide nanofillers. It will help to reach a final conclusion about nanofillers' significance in enhancing fiber matrix bonding properties. Further scope of this study will be to find out the effects of other different nanofillers in enhancement of machining properties of different composite materials and also to find out inter molecular relation of the nanofillers with the fiber and matrix molecules.

1.7 THESIS OUTLINE

The chapters of this thesis are organized by the following manner:

Chapter 2 describes an overview of composite materials and their groups. It includes features and attributes of hybrid composites made of glass and jute fiber. Machinability of composite materials, their earlier investigations and techniques the function of nanofillers in improving machinability and mechanical qualities are also described in chapter 2. An overview of research on the use of nanofiller in composite materials, finding gaps in the body of knowledge and research questions are also adjoined.

Chapter 3 focuses on Material Selection and Preparation, Detailed description of jute and glass fibers and their properties, selection criteria for nanofillers and their properties, manufacturing process of hybrid composite specimens, Methods for nanofiller incorporation and characterization techniques, experimental design for machinability analysis.

Chapter 4 delineates Machinability testing overview of machining processes used in composite materials, description of experimental setup and machining parameters, machinability testing procedures and methodologies, analysis techniques for evaluating machinability parameters, Data collection methods and instrumentation used.

Finally, chapter 5 expounds on results and discussions. It describes Presentation of machinability test results, Analysis of machinability parameters such as surface roughness and delamination, Comparison of machinability of jute and glass fiber hybrid composites with and without different nanofiller incorporation, discussion on the influence of nanofillers on machinability and mechanical properties, interpretation of results in relation to existing literature and research objectives.

Chapter 6 concludes the thesis works based on the experimental findings, as well as conveys the recommendation for future works in this research area.

Chapter 2
Literature Review

2.1 INTRODUCTION

In order to tackle the shortcomings of NFR composites, hybridization with synthetic fibers is a good alternative. Adding nano fillers to composites is another method of improving their qualities. Nanomaterials differ from pure polymers in their mechanical, thermal, optical, electrical, magnetic, and barrier characteristics [20-22]. Nano-sized silica, zinc, alumina, titanium dioxide, calcium carbonate, lead oxide, silicon carbide, carbon black, nano clay, and other types of nanofibrils and cellulose nanocrystals are commonly employed as fillers to reinforce polymer composites. Addition of nanofillers along with the hybridization can further enhance the properties and fiber matrix bonding characteristic of the composite material. The qualities of individual fibers and nanofillers can be tailored through hybridization of natural fibers with nanofillers, which also improves the properties of the resulting composite [23]. Because they are lightweight and less likely to corrode, composites have become popular substitutes for metal alloys in a variety of technical applications [24]. The material weight also drops since there are fewer nanoparticles added than there were in the bulk phase [25]. In order to give a good shape of the composite to enable their usage in certain application, machining is of absolute importance. The fiber-reinforced composites' uppermost portions are molded into roughly net forms, but machining is required to achieve surface quality and dimensional accuracy [26]. The components are assembled using secondary operations such as milling, which removes superfluous material to create a geometric shape, and drilling, which creates holes [27]. Two major factors which should be considered the most important regarding machining of composites are surface roughness and delamination. After producing the net shape of an object, secondary operation like drilling, milling, turning etc. are performed to get the desired finish of the material. However, during machining, the main disadvantages of these composite materials include delamination, surface roughness, microcracks, fiber breakage, and separation of fiber and resin [28]. A good surface finish ensures excellent mating condition for different parts which is determined by surface roughness. Therefore, it is crucial to select the right parameters for multi-axis machining, including feed rate, cutting speed, and lead angle [29]. In this chapter, Previous studies of hybrid and natural fiber composites are discussed. Also previous studies on nanofiller addition, their effects and various tests done for testing machinability of composites are also presented.

2.2 PREVIOUS STUDIES

Thus far, a number of studies on nanocellulose-reinforced composites have been described, demonstrating a notable improvement in performance. Kishore M, Amrita M [23] They also tested the machinability of the produced composite and found that The hybrid composite with 0.4 weight percent graphene (HFC G0.4) at a lower feed value, or 0.5 mm/ rev, has the lowest roughness value. When compared to hybrid composites without graphene, hybrid composite (HFC G0.4) had the greatest reduction in surface roughness, 39% [27]. Akmam Noor Rashid M, Mohd Zain Z studied Machinability study of JFRP composite using design of experiment [30]. They discovered that the most important element influencing the out-of-the-box responses of tool wear, surface roughness, and delamination factor is the machining feed rate. The optimal cutting speed, feed rate, and depth of cut were determined to be 4293.56 revs/min, 150 mm/min, and 1.0 mm, respectively. 1.18 µm was the ideal surface roughness value. When milling kenaf fiber-reinforced composites, a low feed rate results in the least amount of surface roughness, whereas cutting speed has no effect on surface roughness. However, it has been discovered that a product with a superior surface quality is produced with a deeper cut and a faster cutting speed. The best machining conditions for milling woven jute natural fiber composites are said to be high cutting speed, low feed rate, and medium depth of cut in order to achieve superior surface roughness and reduced delamination [31]. Another significant challenge is the heat generated during milling. The heat generated tends to melt the polymer and burn the fiber, causing delamination and fiber peeling [32], even though it can reduce thrust force. The delamination damage can be lessened at lower feed and tip angles. Additionally, spindle speed has a considerable impact on delamination, as do feed rate and tip angle [33].

Many studies have been conducted in recent years to improve the machinability of polymer composites to the level of metal-based composites. The specific properties of the reinforcements and matrix materials affected the cutting forces and damage that occurred in the composite's surface and subsurface. Typically, it is discovered that the drilling process works best with a greater spindle revolution speed, smaller drill diameter, a point angle closer to 1000, a lower tool traverse rate, and a favored parabolic tool drill [34]. Over the past ten or so years, there has been an exponential increase in the quantity of research papers on natural fiber composites. It is true that there are a lot of articles on hybrid composites made of natural and synthetic fibers. All of them will be too many to cover in one chapter. Consequently, only the most pertinent and current research on hybrid composites will be covered in this chapter. This chapter summarizes recent research on the machinability tests and mechanical characteristics of two natural and one synthetic fiber-reinforced hybrid composites. I assessed hybrid composites made using only the hand lay-up approach to show how hybridization and the addition of nanofiller enhance their properties. The impact of bamboo nanoparticles in kenaf fiber-polyester composite was a investigated by E. Rosamah et al [35]. The findings showed that adding 3% of nanofillers improved the composite's mechanical and thermal qualities by strengthening the link and increasing its wettability with the matrix. However, the results also showed that agglomeration caused the composite to deteriorate when a larger percentage of nanoparticles (>3 percent) were added. The mechanical, thermal, morphological, and barrier characteristics of nanocomposites made of PVA and nanocellulose that was separated from leftover sugarcane bagasse were investigated by Arup Mandal et al. [36]. Both crosslinked and linear PVA showed a significant increase in toughness, yield force, tensile strength, and % elongation at break. The reinforced PVA composite's crystalline melting temperature decreased and its thermal stability was notably superior to that of neat PVA. Celik et al. [37] investigated the effects of cutting parameters including feed rate and speed on surface roughness and delamination on jute fiber composites with different orientations using a milling operation. It was found that while the cutting force decreases with increased cutting speed, it increases with increasing feed rate. Surface roughness and delamination factor increase with increasing feed rate for all orientations of the composite, but surface roughness and delamination factor decrease with increasing cutting speed. Babu et al. [38] milled synthetic fiber material, glass, jute, hemp, and banana (natural fiber reinforced material) at three different feeds and speeds. Sikiru Oluwarotimi Ismail, Hom Nath Dhakal studied the drilling properties of hemp composite. The hemp composite has the lowest delamination factor (Fd) and the best surface roughness of all the composites, according to the results [39]. It has been noted that while the speed increases, the Ra value falls and the Ra value increases with an increase in feed rate. A similar pattern with the delamination factor was also seen. As the aspect ratio rose, so was the impact of feed rate on surface roughness and delamination. While the delamination factor increased with an increase in feed rate, it decreased with an increase in cutting speed. As a result, the delamination effect was reduced by low feed rate and high cutting speed. Compared to cutting speed, feed rate has a stronger impact on delamination and surface roughness; surface roughness increased with feed rate, whereas cutting speed had a negligible effect; surface roughness decreased as cutting speed increased. Chetia et al. [40] used analysis of variance (ANOVA) to investigate the impact of feed parameters and speed on basalt/bamboo composite drilling. It was determined that, in comparison to speed, feed had a greater influence on the delamination factor (Fd). One can utilize filler materials to lessen thrust force, delamination, etc. The impact of drilling parameters using filler materials like titanium dioxide was investigated by Murugesh and Sadashivappa. [41](TiO_2) and graphite in varied proportions within the glass fiber and epoxy composites. Due to the abrasive character of these filler elements, their use resulted in a decrease in delamination and a reduction in thrust force. In their attempt to investigate the effects of cutting parameters on surface roughness quality, Rao, G Harii Krishna, Ansari, M N M, and Begum, Shahida discovered that depth of cut is the most important factor, followed by feed rate and spindle speed, which are the medium significant factors. For this specific type of MWCNT Epoxy composite, the most significant interactions that affect surface roughness of machined surfaces were between feed rate and depth of cut [42] . Using an experimental design, Mir Akmam Noor Rashid, Zakaria Mohd Zain, M K Nor Khairusshima, Wazed Ibne Noor, Momin Mullah, and Shaheer Ahmed Khan investigated the machinability of JFRP composite. The most important element influencing the out-of-the-box responses of tool wear, surface roughness, and delamination factor was determined to be the machining feed rate. The optimal cutting speed, feed rate, and depth of cut were determined to be 4293.56 revs/min, 150 mm/min, and 1.0 mm, respectively. 1.18 µm was the ideal surface roughness value [43]. Lotfi A, Li H, and Dao D investigated the machinability analysis of drilling laminates made of polylactic acid bio-composite reinforced with flax fiber. The experimental findings showed that the cutting thrust force and, consequently, drilling-induced damages are significantly impacted by the material and geometry of the cutting tool. High-speed steel (HSS) drills produced lower thrust force values and higher hole quality, while carbide drills, which have a point angle of 130 degrees, produced the greatest thrust force values. While HSS drills demonstrated a lower thrust force value during the drilling process, carbide drills demonstrated greater wear resistance and consistency in the variance of thrust force with the number of holes drilled. Lastly, the delamination damage increased somewhat with spindle speed and significantly with feed rate within the chosen cutting range [44]. Using conventional versus ultrasonically-assisted machining, D Wang, PY Onawumi, SO Ismail, HN Dhakal b, I Popov, VV Silberschmidt, and A Roy investigated the machinability of natural fiber-reinforced polymer composites. Their research focuses on comparing the experimental results of hybrid ultrasonically-assisted drilling (UAD) and conventional drilling (CD) on a hemp fiber-reinforced vinyl ester composite laminate. For a variety of drilling situations, the results show that UAD is more effective than CD. It produces less cutting energy and force, which lessens machining-induced damage to the composite, such as fiber pull-outs and burr development. When compared to CD-produced holes, UAD-drilled holes have better surface finish and hole quality. According to the study, UAD is a practical machining technique that may be used to increase the machinability of heterogeneous NFRP composite materials [45]. Mohamed, El Mansori, Faissal, and Chegdani experimented with a novel multiscale method for machining analysis of bio-composites reinforced with natural fibers. The findings demonstrated that particular analysis scales that are closely related to the natural fiber structure are needed for machining NFRP composites. The multiscale approach can be utilized to enhance the NFRP machining experimental design and, more importantly, to identify the ideal process parameters that take into account the multiscale machining properties of these bio-based materials [46].

Chapter 3

Materials and Method

3.1 INTRODUCTION

A composite is a multi-phase system where one or more attributes are optimized through the intentional tailoring of the geometry and phase distribution. At least two materials with physically separate phases make up composite materials. The term "matrix" refers to a typically continuous phase, whereas "reinforcement" refers to a scattered phase that can be either fibrous or particulate. Sometimes, composite can have better properties than either phase individually because of the way the phases interact. The materials and techniques utilized for the hybrid composites' chemical treatment, manufacture, sample preparation, mechanical testing, and characterization are covered in detail in this chapter.

3.2 MATERIALS

The reinforcing (jute and E-glass fibers) and matrix (resin) ingredients were the two primary composite components utilized in this work, which started with descriptions of the composite material. The following basic components were utilized in the investigation to create the hybrid composite:

1. Jute Fiber
2. Glass Fiber
3. Epoxy & Hardner
4. Nano Particles (TiO_2, ZnO_2, Al_2O_3)

3.2.1 Jute Fiber (Corchorus capsularis)

Jute belongs to the Sparrmanniaceae family of bast fibers. It comes from two herbaceous annual plants: Corchorusolitorius (Tossa jute), which comes from Africa, and white Corchoruscapsularis (white jute), which comes from Asia. Of the more than thirty species of Corchorus, the most well-known is the white jute (Corchorus capsularis) [36]. Bundles of jute fibers are made up of several fibers that are joined by non-cellulosic materials, primarily lignin and pectin. The processes of retting, stripping, or decortication are used to remove the fibers from the stem. During the season, jute takes almost three months to reach a height of 12 to 15 feet. After that, it is chopped, packed, and submerged in water for the "Retting" process, which separates the inner and outside stems and "individualizes" the outer plant to create fiber. After that, the plant is separated and cleaned to get rid of any dust. Following drying, the fiber is sent to jute mills where it is transformed into jute yarn and hessian.Jute fiber extracted from the bark of the jute plant has three major categories of chemical compounds, namely cellulose (58–63 wt%), hemicellulose (20– 24 wt%) and lignin (12–15 wt%) and some other small quantities of components like fats, pectin's and aqueous extracts.

Because of its somewhat high specific strength and stiffness, it can be used as reinforcement. Its application in polymer composites has increased due to its affordability and availability [37]. It does, however, show significant diversity in both diameter and filament length. Size, maturity, and the processing techniques used for fiber extraction all affect the fiber's characteristics The interior structure and chemical makeup of the fiber affect its properties, including density, electrical resistivity, ultimate tensile strength, and initial modulus. Known as Bangladesh's "golden fabric," jute has drawn a lot of interest in the composites industry as an environmentally friendly reinforcement. For the past 10 years, it has been utilized in many everyday applications, including as bags, beds, and ropes. Jute comes in a variety of forms:

1) Raw Jute

2) Jute Fiber

3) Woven Jute Fiber Mat

Figure 3.1 shows the raw jute mat used in this research where the fiber direction was cross-ply. Typical physical and mechanical properties of jute fiber are listed in Table 3.1 and Table 3.2. Jute woven fabrics and GFRP were taken and cut according to the length of the specimen and weighed using a precision balance. After that, the fibers were cleaned with pressured water to get rid of any undesired organic elements that were on the surface. They were then let to dry in the sun for eight hours to get rid of any remaining moisture.

Figure 3.1: Untreated bi-directional jute mat

Table 3.1: Mechanical properties of jute fiber

Tensile Strength (MPa)	Specific Tensile Strength (MPa)	Young's Modulus (GPa)	Specific Young's Modulus (GPa)	Failure Strain (%)
200-450	140-320	20-55	14-39	2-3

Table 3.2: Physical properties and composition of jute fiber

Property	Value	Property	Value
Density (g/cm^3)	1.4	% Elongation	1.5–1.8
Diameter (mm)	25.2	Cellulous content (%)	58–63
Tensile strength (MPa)	393–773	Hemicelluloses (%)	12
Tensile modulus (GPa)	10–30	Lignin content (%)	12–14

3.2.2 Glass fiber

Glass fiber is an extremely versatile material due to its inherent strength, weather-resistant finish, lightweight nature, and variety of surface textures [97]. The fibers can be randomly placed, flattened into a sheet called a chopped strand mat, or woven into glass fabric. The most common type of glass fiber in fiberglass is called e-glass, an alumina-borosilicate glass that contains less than 1% w/w alkali oxides and is mostly used for glass-reinforced plastics. E-CR-glass, an alkali-lime silicate with less than 1% w/w alkali oxides and a strong acid resistance, and A-glass, an alkali-lime glass with little to no boron oxide, are other forms of glass that are utilized. R-glass is aluminum silicate glass without MgO and CaO with high mechanical requirements as reinforcement; S-glass is aluminum silicate glass without CaO but with a high MgO content and high tensile strength; C-glass is alkali-lime glass with a high boron oxide content and is used for insulation and glass staple fibers; and D-glass is borosilicate glass due to its low dielectric constant [98]. Among the fascinating properties of fiber reinforced plastic (FRP) composites are their high specific strength and stiffness, good fatigue performance and damage tolerances, low thermal expansion, non-magnetic properties, corrosion resistance, and low fabrication energy consumption [99]. Table 3.3 lists important characteristics of glass fiber reinforced composite materials.

Table 3.3: Properties of glass fiber reinforced composites

Material	Specific gravity	Tensile strength (MPa)	Compressive strength (MPa)
E-Glass Epoxy composite	1.99	1,770	
Polyester and Woven Rovings Laminate 45% E-glass	1.6	250	150
Polyester and Continuous Rovings Laminate 70% E-glass	1.9	800	350
Polyester and Chopped Strand Mat Laminate 30% E-glass	1.4	100	150
Polyester and Satin Weave Cloth Laminate 55% E-glass	1.7	300	250

Polyester and Continuous Rovings Laminate 70% E-glass	1.9	800	350
S-Glass Epoxy composite	1.95	2,358	

In the present study, randomly oriented glass fiber mat is used, depicted in Figure 3.2. Properties of the used E-glass fiber are listed in Table 3.4.

Figure 3.2: Glass fiber mat

Table 3.4: Properties of fiberglass

Material	Specific gravity	Tensile strength MPa (ksi)	Compressive strength MPa (ksi)
Polyester resin (Not reinforced)	1.28	55 (7.98)	140 (20.3)
E-Glass Epoxy composite	1.99	1,770 (257)	
Polyester and Woven Rovings Laminate 45% E-glass	1.6	250 (36.3)	150 (21.8)
Polyester and Continuous Rovings Laminate 70% E-glass	1.9	800 (116)	350 (50.8)
Polyester and Chopped Strand Mat Laminate 30% E-glass	1.4	100 (14.5)	150 (21.8)
Polyester and Satin Weave Cloth Laminate 55% E-glass	1.7	300 (43.5)	250 (36.3)
Polyester and Continuous Rovings Laminate 70% E-glass	1.9	800 (116)	350 (50.8)
S-Glass Epoxy composite	1.95	2,358 (342)	

3.2.3 Epoxy Resin and Hardener

The selection of a resin system depends on the following properties for most composite structures:

- Adhesive Properties
- Mechanical Properties
- Micro-Cracking resistance
- Fatigue Resistance

Epoxy compounds are defined by an oxirane or epoxy ring, which is a three-membered ring with an oxygen atom attached to two carbon atoms that had previously been connected in some other manner. Epoxy resin is composed of epoxide groups at each end of monomers or short-chain polymers..

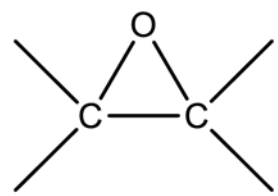

Figure 3.3: epoxy ring

This thermosetting polymer is the result of a reaction between an epoxide "resin" and a polyamine "hardener". Epoxy comes in liquid and solid forms and is cured into the final plastics by a catalyst. They are cured at room temperature as well as at higher temperatures. Its cost-performance ratio is outstanding. Epoxy's characteristics include:

- Outstanding resistance to chemicals, especially in alkaline settings.
- Outstanding adherence to a range of substrates and exceptional chemical resistance, especially in alkaline settings.
- Compressive, flexural, and tensile strengths are exceptionally high.
- Minimal shrinking after curing.

- Exceptional ability to withstand corrosion.
- The ability to heal at different temperatures and a strong resistance to physical injury.
- The capacity to cure at a variety of temperatures.
- Exceptional resilience to fatigue.

outstanding resilience to fatigue.It takes a hardener for each epoxy to begin the curing process. The catalyst is another name for the substance that hardens the adhesive when mixed with resin. When the hardener and resin combine, the hardener opens the C—O—C rings, rearranging the connections to bring the monomers together form a three-dimensional network of molecules that resembles crosslinked chains. Some epoxy resins cure rapidly at room temperature, but many high-strength epoxy resins need to cure at a higher temperature. The hardener is composed of polyamine monomers. Because polyamines and acid anhydrides can provide extremely active groups, a minimal amount of these substances is all that is needed to participate in the system's curing and completely cure it, making them the most widely employed curing agents. The addition principle, which underlies the entire curing process, can be used to add them directly. When these molecules' amine and epoxide groups come together, a covalent link is formed. Each and every NH group can react with an epoxide group to create a rigid, robust, and crosslinked polymer. The polymerization or "curing" process can be impacted by temperature, resin type, and hardener choice. The process could take a few minutes to several hours.

The final properties and appropriateness of the epoxy for the specified environment are determined by the choice and combination of the resin and hardener. Because it will influence the chemical reaction, pot life, and final material qualities, the curing agent should be carefully chosen.

Table 3.5: Properties of epoxy and hardener

Properties	Epoxy resin	Hardener
Appearance	Clear liquid	–
Viscosity at 25°C (mPa s)	10,000–12,000	50–100
Density (g/cm^3)	1.15–1.20	1.20–1.25
Tensile strength (MPa)	83–93	–
Tensile modulus (GPa)	0.3–0.6	–

Figure 3.4: Epoxy and hardener

To start the curing process, epoxy resin needs a hardener, also known as a catalyst, which solidifies the glue and starts an exothermic reaction that produces heat. The final properties and appropriateness of the epoxy coating for the specified environment are determined by the particular choice and mix of the epoxy and hardener. Only when the hardener and epoxy resin are accurately measured according to a prescribed ratio, combined thoroughly, and the temperature and humidity are optimal can a proper cure occur. The extra resin is inefficient, adds weight, and does not increase strength.

The resin and nano fillers are combined first, followed by the hardener, to form the polymer matrix. The ratio of resin to hardener was kept at 10:1. Since this is a whole chemical reaction and all of the components must react completely for the matrix to have optimum strength, it is crucial to adhere to the correct proportions, which can be determined by weight or volume.

A glass rod or stirrer and a beaker were taken and thoroughly cleaned with warm water and running water. Next, a breaker was filled with the determined amount of epoxy resin and nanoparticles. After 30 minutes of constant, thorough mixing with a beater, a measured amount of hardener was added to the mixer. Nano fillers made up 3 weight percent of the total. This stirring was done in order to make the mixture homogenous. Using the typical laboratory data listed in the chart, the pot life of epoxy was determined to be 20 minutes.

3.2.4 Nanoparticle synthesis

In this work, three types of inorganic nanoparticles—Al_2O_3, ZnO, and TiO_2—were employed. They were bought from Taj Scientific Stores in Chittagong, Bangladesh, in micron size.

Aluminum oxide (Al_2O_3), the hardest form of alumina, is commonly used as a filler to improve the mechanical and thermal properties of polymers [101]. Al_2O_3 is one of the most widely used engineered ceramic materials because of its high elastic modulus, strong wear resistance, high chemical corrosion resistance, high-temperature stability, and capacity to retain strength at high temperatures [102].

One of the most widely used nanoscale inorganic fillers in polymer nanocomposites is zinc oxide nanopowder (ZnO). ZnO enhances the composite's mechanical, UV, thermal, and other relevant properties [88]. Polymer-ZnO composites have been studied as technologically significant due to their potential applications in solar cells, electrochromic windows, optical devices, gas sensing, varistors, piezoelectric devices, electro-acoustic transducers, photodiodes, UV light-emitting devices, photo stabilizers, and in the antimicrobial application of food preservation. The use of ZnO nanoparticles in composites made of polymers shows great promise. Currently, one of the most intriguing materials is titanium oxide nanoparticles. As they continue to be developed, they are gaining more and more attention due to their special qualities as well as their possible uses in sectors like pigments, cosmetics, catalysts, photocatalysts, etc. Table 3.6 lists the particle's characteristics.

Table 3.6: Properties of the various metal oxide particles used in this study.

Metal oxide	**Properties**
Aluminum oxide	Molecular weight: 101.96
	PH value: 6.5-7.5
	Wt. per ml (approximately): 0.9g
	Particle size: 70-230 mesh
Zinc oxide	Molecular Weight 81.39 g/mol
	Assay (complexometric): Min. 98.0%
	Maximum Limits of Impurities: Chloride (Cl): 0.005%
	Sulphate (as SO_4): 0.02 %
	Arsenic (As): 0.0005%
	Lead (Pb): 0.005%
	Iron (Fe) 0,001%
	Substances reducing KMn O_4 (as O): 0.001%

	Loss on ignition (500℃) 1.0 %
Titanium dioxide 	Molecular Weight 79.87 g/mol
	Assay (complexometric): Min. 99.0%
	Substances soluble in water 0.5%
	substances soluble in diluted HCL: 0.5%
	Maximum Limits of Impurities: Sulphate (as SO_4): 0.05 %
	Heavy metals (Pb): 0.003%
	Iron (Fe) 0,005%
	Arsenic (As) 0.0005%

A ball mill is a grinding device commonly employed for the purpose of reducing bulk material into particles of nano-scale dimensions. This is achieved through the utilization of zirconium or steel balls of varying sizes, which facilitate the grinding and blending process. The reduction in size is accomplished through a combination of impact and attrition as the ball falls from near the top of a revolving hollow cylindrical shell. All these oxides are ball milled at a speed of 450 rpm for about 1 hour to achieve the nano-size. After milling a strainer was used to collect the particle in a glass jar. The powder was preserved in a vacuum desiccator for an inert environment. Figure 3.5 depicts the image of the ball milling machine used in this study.

Figure 3.5: Ball milling machine

3.3 CHEMICAL MODIFICATION OF JUTE FIBER

A major factor in describing the mechanical characteristics of the composites is the interfacial adhesion between the fiber and matrix. Poor adhesion at the phase boundary causes a relatively weak force dispersion, which impairs the mechanical properties of the composite. A well-designed interface greatly increases the strength of composites, provides structural stability, and ensures effective load transfer from matrix to reinforcement, all of which help to lessen stress absorption. The natural lignocellulosic fibers absorb moisture and are hydrophilic. The plant fiber cell wall contains a large number of hydrogen bonds (hydroxyl groups, or -OH) between the macromolecules. The hydrogen link breaks and new hydrogen bonds are formed between hydroxyl groups and water molecules when atmospheric moisture comes into contact with the fiber. The main route to the penetrating water is the fiber's cross-section. Consequently, when hydrophilic fiber is reinforced with hydrophobic resin, the fiber swells inside the matrix, leading to poor mechanical characteristics of the composites, dimensional instability, matrix cracking, and weak fiber-matrix bonding [106]. Thus, removing moisture from fibers is a crucial step before composites are prepared. To improve the efficiency of interfacial bonding, the fiber surface is modified using various chemical treatments. Reinforcing fiber that has been chemically treated has a decreased hydrophilic inclination and is therefore more compatible with the matrix. By altering the fiber element's composition to interact with the matrix, it uses a hydroxyl group to activate the fiber structure [107]. Consequently, the fiber-reinforced composite's mechanical qualities and strength are enhanced due to improved adhesion between the fiber surface and polymer matrix. Every chemical treatment has benefits and drawbacks of its own. Alkaline treatment is the most widely used technique for altering the fiber surface.

- ALKALINE TREATMENT

The most popular technique for enhancing fiber-matrix adhesion and eliminating both natural and synthetic contaminants is alkali treatment, also known as mercerization. Additionally, it aids in decreasing the fiber diameter, which raises the aspect ratio. Better fiber-matrix interface adhesion, improved mechanical interlocking, and cellulose exposure on the fiber surface are all made possible by the development of a rough surface and an increase in aspect ratio. These factors also increase the number of potential reaction sites and facilitate better fiber wetting.

Alkali Treatment: Alkali is applied to natural fibers by rinsing them in a NaOH solution for a full day and then washing them with water. The removal of wax and fatty materials by a NaOH solution alters the fibers' surface topography, causing fibrillation and the disintegration of fiber bundles into smaller fibers. Figure 3.8 depicts the reaction that occurs during this treatment.

$$Fiber - OH + NaOH \rightarrow Fiber - O - Na + H_2O$$

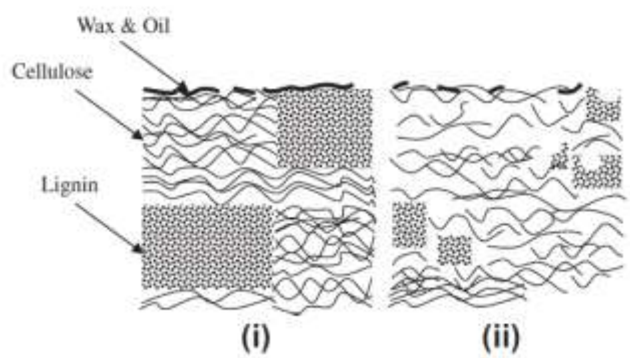

Figure 3.6: Typical structure of (i) untreated and (ii) alkalized cellulose fibre

The main alteration caused by the NaOH solvent is the breaking of hydrogen bonds in the network structure, which also depolymerizes cellulose, exposes the short-length crystallites, and removes a certain amount of lignin, wax, and oils from the fiber cell divider's exterior surface. It shifts the orientation of the densely packed crystalline cellulose order, creating an amorphous area, and accelerates the ionization of the hydroxyl social event to the alkoxide. Alkaline therapy affects the fiber in two ways, to put it briefly:

- It improves mechanical interlocking by increasing surface roughness.
- Because of this, there are more cellulose molecules that are exposed on the fiber surface.

During this process, the concentration of the NaOH solution, the operating temperature, the length of the treatment, the strength of the material, and the additives used are all taken into account [96]. The relationship between sodium hydroxide (NaOH) and natural fiber and natural fiber-reinforced composite was examined by a number of researchers. Their findings demonstrated that alkali treatment had a direct and widespread impact on the thermal and mechanical properties of NFC, eliminating both artificial and natural impurities to produce a rough surface topography.

T Many contaminants are typically present in freshly pulled fibers, which might negatively impact the fiber matrix bonding. As a result, the composite material composed of these fibers might not have mechanical qualities that are satisfactory. To achieve a better fiber-matrix connection, it is therefore preferable to remove the fibers' impurity content and maybe improve their surface topography.

Natural fiber incompatibility results in low fiber-matrix interfacial binding strength and inadequate matrix resin wetting of the fibers, which impairs the composites' mechanical qualities. Because of cellulose and lignin, jute fibers contain a hydroxyl group. This hydroxyl group lowers the activity towards the matrix by forming hydrogen bonds within the cellulose. However, these disadvantages are generally lessened by surface alterations either chemically or physically. Alkaline treatment is thus used to increase the fiber matrix adherence and strength of the natural fiber composite.

The fibers' strength is increased through chemical treatment with NaOH, which eliminates their moisture content. Additionally, it stabilizes the molecular orientation, removes all contaminants that are adjacent to the fiber material, and increases the flexural rigidity of the fibers. In order to properly de-polymerize cellulose, hemicellulose, pectin, and lignin, the jute fibers were alkalized by soaking them separately in a 5% (w/v) aqueous alkaline (NaOH) solution at room temperature for 24 hours while being stirred intermittently. The fibers: solution ratio was kept at 1:15 (w/w). About 41% of the hemicellulose cementing material in the fiber structure is removed as a result of the alkali treatment's swelling of the fibers' amorphous areas. Following soaking, the fibers were repeatedly rinsed with distilled water to get rid of any extra NaOH that had adhered to their surface. A pH paper was used to confirm the fibers' neutrality, and they were then thoroughly rinsed with distilled water until they were clear of alkali. Seven was the final pH that was maintained. The fibers were then dried for hours in the sun or open air and then for eight hours at 100 degrees Celsius in an oven.


(a)


(c)


(b)


(d)

Figure 3.7: (a) Jute fiber soaked in NaOH, (b) Distilled Water (c) Drying the fibers in sunlight (d) in Woven

3.4 COMPOSITE FABRICATION

Various researchers have employed different composite fabrication methods to achieve goal or specific property improvement. The size and shape of the final composites, the intended attributes, the raw material processing properties, production speed, and manufacturing cost are some of the factors that influence the choice of fabrication process. The most common technique for thermoset composites, particularly among researchers, is hand layup. This method's easier fabrication process has led to numerous investigations favoring it.

Hand lay-up is a molding approach wherein reinforcements are positioned by way of hand, and then polymer resin is poured at the fiber reinforcement. The method's initial step is to prepare a mold according to the final product's required structure. Mold can be made of any material like iron, wood, plastic, Paris, etc., depending upon the processing cost. Paris mold may break during the release of the product. Wood mold needs to be completed at each molding cycle. Glass steel mold is ideal for complex shapes. Metal molds are preferred when heating and pressing are required. There are distinct steps at the beginning of the process. As resins are highly viscous, the product may stick to the mold, and product release can be affected. Few released gels are added on the mold’s surface to avoid any adhering of composite constituents on the surface. Thin plastic sheets are used and covered the mold’s top and bottom to get samples with a smooth surface. For improved and highly eminent texture, pigmented gel coat is applied on the surface of the mold. It is usually a thin layer of resin that is about several mm on the product's surface. It creates an outer layer of the completed part that is both attractive and protective. Once the gel coat has solidified enough to resist solvent attack from the laminating resin, laying up can begin.

Reinforcements in woven, knitted, stitched, or bonded fabrics are cut as per the mold size and placed at the mold’s surface. Fibers can be oriented in different configurations according to the required design. The resin in liquid form is mixed with a hardener (liquid form) in suitable proportions and then applied over the layers by pouring or spraying. Impregnations of the fibers are done with the help of a brush and roller. Brushes are used to spread the resin uniformly inside the mold. Rolling operations with mild pressure help squeeze out the extra resin, remove the excess air bubbles, and consolidate the laminate. Fiber reinforcements are applied in successive levels until the necessary number of layers is stacked. Until the necessary composite part is completely created, these processes are repeated by applying a new layer on top of the previous layer.

In other cases, the procedure can call for a few extra materials to make the composites more rigid. Therefore, low-density core materials like foam, honeycomb, and End Grain Balsa are frequently employed to stiffen the laminate. Sandwich construction is another name for this method. After achieving the desired thickness, the composite is lightly rolled before curing, and a releasing sheet is placed on top to shield its surface from the elements. After fabrication of composite, the sample is allowed to cure either at room temperature or some specific temperature. The time of curing depends on the type of polymer used for composite processing. For example, the standard curing time at room temperature is 24-48 hours for the epoxy-based system. When the composites are dried to solid, demolding operation occurs where the molds are removed, and the developed composite part is taken out and further processed.

3.5 MOLD PREPARATION

In this experiment a mold was made of wood in dimensions 500 mm × 500 mm. Adequate mold preparations were completed prior to the lay-up procedure commencing. Using an abrasive paper, the base plate was scrubbed to remove rust. After cleaning the surface with acetone and lint-free towels to get rid of any oil, grease, or grime, it was let to dry. Following drying, a mold release sheet and mold release spray were applied to the top and bottom of the wooden mold to facilitate the rapid and simple removal of the composite material. When laminates are separated, mold release is necessary to keep the epoxy from adhering to the mold. In order to achieve this, a Mylar sheet is positioned over the lower portion of the mold to provide a smooth surface finish and facilitate the simple removal of the composite from the mold. Additionally, the surface of the Mylar sheet is covered with wax to facilitate the removal of the composite. The superb releasing qualities, simplicity of application, and remarkable mirror finish shine of Mold releasing silicone spray led to its selection.

Figure 3.8 Wax & Mylar paper

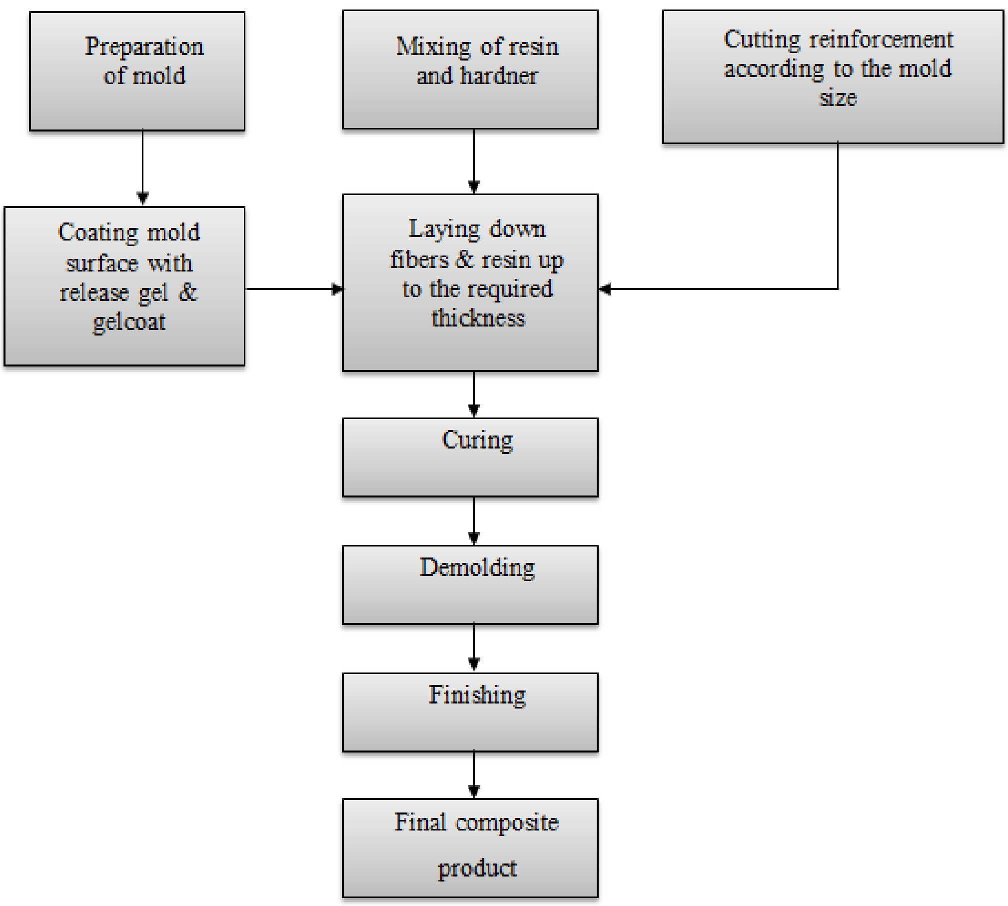

Figure 3.9: Technique flow chart of hand layup method

3.6 MATRIX PREPARATION

In order to create composites, this study used glass fiber and jute as reinforcement inside an epoxy matrix and three distinct nanoparticles as additives. The weight percentage ratio of reinforcement to polymer matrix was kept at 40:60. Fiber-reinforced hybrid composites were made for this experiment at room temperature with an average relative humidity of 65%. releasing qualities, convenience of use, and remarkable luster of the mirror finish.

3.7 FABRICATION OF THE SPECIMEN

First, emery paper must be used to scrub the mold clean. After cleaning the surface with a thin solution, the surface was left to dry before the mold was sprayed to make the specimen easy to remove. After thoroughly mixing epoxy, nanoparticles, and hardener, the mixture was put onto mylar paper and applied to a section using a paintbrush. After that, a single piece of glass cloth was laid out on top of the epoxy resin mixture and manually rolled. The roller was used to remove trapped air and distribute epoxy uniformly. More resin can be applied on top and spread out if the fiber is not entirely wet. At this point, the second layer of fiber, or jute mat, was applied, and extra care was taken to ensure that there were no air bubbles. The roller was used to push out the air spaces that developed between the layers. We refer to this process as consolidation or compaction. The appropriate fibers were used to fill the successive layers before the glue dried. A squeegee or flexible plastic spreader was used to uniformly disperse the resin and remove surplus resin until the material was saturated after the fiber layers were sandwiched between two sheets of mylar paper. The fiber stacking sequence G/J/J/G was maintained for every sample.

Following the placement of the plastic sheet, the inner surface of the top mold plate was sprayed with release gel and left on top of the stacked layers. The whole composite was fastened at all ends and sealed with wooden reapers. Lastly, for the ideal setting, a 25 kilogram rectangular iron bar with the same cross-section was set up on the above assembly for a full day. At normal temperature, an epoxy-based system typically takes 24 to 48 hours to cure. The generated composite portion was removed and subjected to additional processing after the mold was opened after curing. Following construction, the composite specimen was exposed to sunshine for a number of hours in order to eliminate any remaining moisture. The composites' extraneous edges were removed by a grinding machine.

Figure 3.10: Weight for compressing the specimen

Figure 3.11: Samples after Fabrication

3.8 MACHINABILITY ANALYSIS OF COMPOSITES

For machinability analysis response surface methodology with central composite design was used using Minitab 2019 software. For Machinability analysis, following equipment's were used:

1. Semi-Automatic Milling Machine: Maximart MX B5IV
2. Semi-Automatic drilling machine
3. Taylor Hobson Ametek Surface roughness analyzer

Figure 3.12 : Maximart B5IV CNC Milling Machine

Figure 3.13: Taylor Hobson Ametex Surface roughness tester

In order to prepare the samples for analysis, 10mm grooves were cut into each astm standard samples using the cnc milling machine. The number of grooves and their milling criteria were maintained according to the design of experiment which is discussed in the next chapter. Taylor hobson surface roughness tester was used to measure the surface roughness of each milled grooves. Data was recorded in a flash drive.

Figure 3.14: Milling operation

Figure 3.15: Surface roughness measurement

Machinability analysis is a method used to assess how easily a material can be machined to meet the desired specifications. It involves evaluating various aspects of machining performance to determine the most effective and efficient conditions for cutting or shaping a material. The goal is to optimize machining processes to achieve high-quality results while minimizing costs and tool wear. The main factors that affect the machining properties of a composite material are feed rate, cutting speed and depth of cut. In this study these three factors were analyzed to get the lowest surface roughness and delamination while machining. In order to achieve the desired machining performance, the optimal combination of cutting speed, feed rate, and depth of cut was determined using response surface approach. The process of creating, organizing, and evaluating the experiment is known as the design of the experiment. This experiment software design allows for the efficient and effective drawing of the goal, conclusion, and legitimate result. have been carried out to investigate the machinability of FRP and examine the contributing elements. One crucial strategy for developing and refining a statistical model is response surface methodology (RSM). Analysis of Variance (ANOVA) scrutiny tests are used to illustrate the advanced model's performance. Response surface methodology (RSM) is a set of statistical and mathematical modeling tools that help with process development, optimization, and enhancement. The measured output is the response (surface roughness and delamination factor). The parameters being examined are the elements or variables (depth of cut, feed rate, and spindle speed). In order to investigate the relationships between the input components and the measured responses, this study used RSM and analysis of variance (ANOVA). The response data was analyzed using RSM's central composite technique. Prior to applying the RSM to examine the data, the full factorial design of experiments was utilized as an initial step to assess the significance of the parameters on the flaws using Analysis of Variance (ANOVA).

Sequential steps of machinability test are:

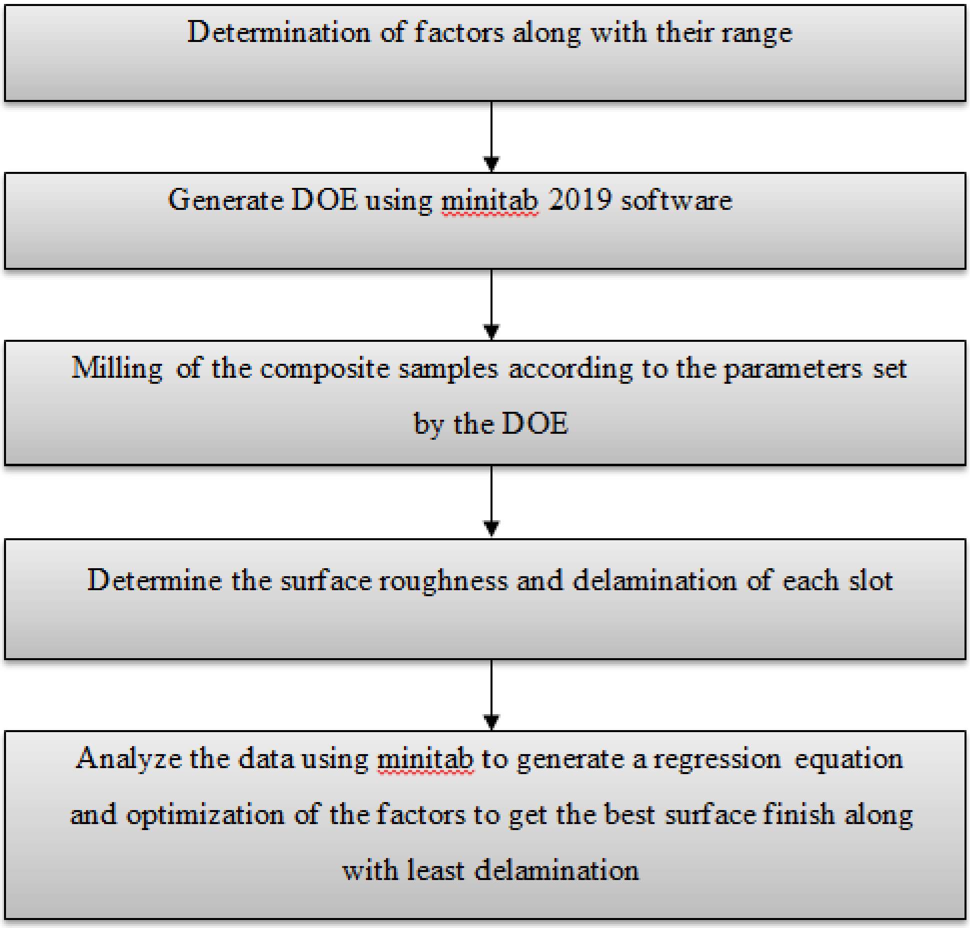

Figure 3.16: Steps of machinability testing.

3.9 MACHINABILITY PROPERTIIES

When testing the machinability of composite materials like jute and glass fiber hybrid composites with nanofiller incorporation, several factors should be analyzed to assess their performance during machining processes. These factors include cutting forces, surface roughness, delamination, tool wear, burr formation, vibration and stability, residual stresses, chip formation and morphology, debonding and fiber matrix interaction etc. Among these factors Surface roughness and delamination has been analyzed in this study as these two has the most effect in post processing of the material.

3.9.1 Surface roughness

Surface roughness refers to the microscopic irregularities or deviations on the surface of a material after it has undergone a machining process. These irregularities are often due to the cutting tool's interactions with the material's microstructure. It is a critical factor in evaluating the quality of a machined surface, particularly in composite materials like jute and glass fiber hybrid composites. It directly impacts the performance, aesthetics, and functionality of the final product. Surface roughness affects various properties of the component, including friction, wear resistance, fatigue strength, and the ability to form seals. In composite materials, it is especially important as it can influence the bonding between layers or components, and the overall structural integrity. Measurement Techniques of surface roughness are :

Contact Methods:

- **Stylus Profilometer:** A diamond-tipped stylus traces the surface, and the vertical movements of the stylus are recorded to create a surface profile. This method is highly accurate but may cause damage to delicate surfaces.

Non-contact Methods:

- **Optical Profilometry:** Uses light, often laser-based, to scan the surface. It is non-destructive and suitable for sensitive materials.
- **Interferometry:** This method uses the interference of light waves to measure surface roughness with high precision. It is ideal for very smooth surfaces.
- **Atomic Force Microscopy (AFM):** A sharp tip scans the surface at the atomic level, providing extremely high-resolution measurements. It is used for very fine surface analysis.

There are several factors that affect the surface roughness in composites such as material properties, machining parameters, tool wear, cooling and lubrication and nanofiller incorporation. Composites present unique challenges due to the heterogeneous nature of the material. The difference in hardness between fibers and the matrix can lead to uneven cutting, causing variations in surface roughness. In fiber-reinforced composites, the orientation of fibers relative to the cutting direction can lead to anisotropic surface roughness. For instance, machining perpendicular to fibers often results in a rougher surface compared to parallel cutting. In fiber-reinforced composites, the orientation of fibers relative to the cutting direction can lead to anisotropic surface roughness. For instance, machining perpendicular to fibers often results in a rougher surface compared to parallel cutting. The incorporation of nanofillers can enhance the surface quality by improving the material's toughness and reducing tool wear, which helps achieve a smoother finish.

Surface roughness can affect the mechanical properties of the composite, such as fatigue resistance and load-bearing capacity, making it critical for structural applications. In products where appearance is important, like automotive or aerospace components, a low surface roughness is essential for a high-quality finish. In multi-layer composites or assemblies, smoother surfaces can improve bonding strength and reduce the risk of debonding. Optimization strategies to control the surface roughness of the composites are tool selection, machining condition and control of nanofiller incorporation. By understanding and controlling surface roughness, manufacturers can improve the quality and performance of machined components made from jute and glass fiber hybrid composites with nanofiller incorporation.

3.9.2 Delamination

Delamination is the process where the bonded layers within a composite material separate or detach from one another, leading to a reduction in the structural integrity and performance of the composite. Delamination is a critical failure mode in composite materials, particularly in fiber-reinforced composites like jute and glass fiber hybrids. It refers to the separation or splitting of the layers within a composite material, often occurring along the interface between the different plies or layers of reinforcement. It is a major concern in composite materials because it can severely compromise the mechanical properties, such as strength, stiffness, and fatigue resistance. In critical applications like aerospace, automotive, and marine industries, delamination can lead to catastrophic failures. Causes behind delamination are:

- High mechanical loads, impact, or excessive vibrations during machining or in-service can induce delamination by causing interlaminar shear stresses that exceed the bonding strength between layers.

- Uneven heating during manufacturing processes or due to environmental conditions can create thermal gradients, leading to differential expansion and contraction of the layers, which may cause delamination.
- Inadequate bonding during the fabrication process, such as poor resin impregnation, voids, or air bubbles, can weaken the interlaminar bond and make the composite more susceptible to delamination.
- Machining operations, especially drilling, cutting, or milling, can induce delamination if improper techniques are used. The interaction between the cutting tool and the composite material can create stresses that lead to layer separation.
- Exposure to moisture, chemicals, or UV radiation can degrade the matrix material or the fiber-matrix interface, leading to delamination over time.

Delamination is a common problem during drilling, especially at the entry and exit points of the drill. It occurs due to the thrust forces generated by the drill bit, which can cause the layers to separate. Improper tool selection or machining parameters can lead to delamination along the cut edges. The interaction between the tool and the composite can generate stresses that cause the layers to peel away. The orientation of fibers relative to the cutting direction affects delamination. For instance, fibers aligned perpendicular to the cutting direction are more likely to cause delamination than fibers aligned parallel to it. Careful selection of cutting speed, feed rate, and tool geometry can minimize the risk of delamination during machining. Lower cutting speeds and smaller feed rates can reduce the forces that cause layer separation.

3.9.3 Delamination Factor (F_d):

$F_d = D_{max} / D$

F_d : Delamination factor (dimensionless).

D_{max}: Maximum diameter of the delaminated area (mm).

D: Nominal diameter of the hole or the intended diameter of the hole (mm).

Interpretation:

- **F_d=1**: Indicates no delamination, as the delaminated area is equal to the nominal area.
- **F_d>1**: Indicates the presence of delamination, with higher values representing more severe delamination.

Chapter 4
RESULTS AND DISCUSSIONS

4.1 INTRODUCTION

In order to conduct the machinability analysis of the samples, response surface methodology is used to design the experiment by using MINITAB 2019. Central composite design is chosen which provided 15 experiments to be conducted.

4.2 DOE AND PARAMETERS

The lower and higher values of cutting parameters are shown in Table 4.1.

Table 4.1: Design parameters

Input Parameter	Highest value	Lowest value
Cutting Speed (rpm)	3000	1000
Feed rate (mm/min)	203	93
Depth of cut (mm)	4	2

Full factorial design with six central points and six axial points is chosen for face centered central composite design which provided twenty experiments for each sample.

Figure 4.1: Parameters of the central composite design

4.3 MACHINING ANALYSIS OF HYBRID COMPOSITE WITH Al_2O_3 NANOFILLER

4.3.1 Delamination

Table 4.2 presents the results of machining for delamination using screening parameters. All the test runs are provided by the design of experiments by using response surface methodology.

Table 4.2 Result for surface roughness and delamination of hybrid composite using Al_2O_3 as nanofillers

StdOrder	RunOrder	PtType	Blocks	Cutting speed	Feed rate	Depth of cut	Ra(Al oxide)	Fd
1	5	1	1	1000	93	2	8.0	1.15
2	13	1	1	3000	93	2	6.9	1.10
3	2	1	1	1000	203	2	10.7	1.34
4	4	1	1	3000	203	2	9.3	1.25
5	12	1	1	1000	93	4	7.9	1.14
6	17	1	1	3000	93	4	6.5	1.09
7	15	1	1	1000	203	4	10.5	1.30
8	9	1	1	3000	203	4	10.2	1.26
9	6	-1	1	1000	148	3	9.2	1.20
10	19	-1	1	3000	148	3	9.0	1.17
11	10	-1	1	2000	93	3	7.5	1.12
12	3	-1	1	2000	203	3	9.9	1.29
13	20	-1	1	2000	148	2	9.9	1.23
14	16	-1	1	2000	148	4	9.5	1.24
15	8	0	1	2000	148	3	9.3	1.23
16	18	0	1	2000	148	3	9.7	1.22
17	1	0	1	2000	148	3	9.6	1.23
18	11	0	1	2000	148	3	9.0	1.25
19	7	0	1	2000	148	3	9.1	1.24
20	14	0	1	2000	148	3	9.2	1.22

Coded Coefficients

Term	Coef	SE Coef	T-Value	P-Value	VIF
Constant	1.22412	0.00497	246.51	0.000	
Cutting speed	-0.02600	0.00468	-5.55	0.000	1.00
Feed rate	0.08400	0.00468	17.94	0.000	1.00
Depth of cut	-0.00400	0.00468	-0.85	0.407	1.00
Cutting speed*Cutting speed	-0.03562	0.00828	-4.30	0.001	1.56
Depth of cut*Depth of cut	0.01438	0.00828	1.74	0.104	1.56

Model Summary

S	R-sq	R-sq(adj)	R-sq(pred)
0.0148053	96.38%	95.09%	92.66%

Analysis of Variance

Source	DF	Adj SS	Adj MS	F-Value	P-Value
Model	5	0.081786	0.016357	74.62	0.000
Linear	3	0.077480	0.025827	117.82	0.000
Cutting speed	1	0.006760	0.006760	30.84	0.000
Feed rate	1	0.070560	0.070560	321.90	0.000
Depth of cut	1	0.000160	0.000160	0.73	0.407
Square	2	0.004306	0.002153	9.82	0.002
Cutting speed*Cutting speed	1	0.004061	0.004061	18.53	0.001
Depth of cut*Depth of cut	1	0.000661	0.000661	3.02	0.104
Error	14	0.003069	0.000219		
Lack-of-Fit	9	0.002385	0.000265	1.94	0.241
Pure Error	5	0.000683	0.000137		
Total	19	0.084855			

Figure 4.2: Machinability analysis of delamination for hybrid composite using Al_2O_3 as nanofillers

The experiment is done considering 95% confidence level. That indicates any P value less than 0.05 indicates that factor is significant. From Figure 4.2 it can be deducted that both cutting speed and feed rate are significant which has most effect on delamination. Lack of fit 0.241 indicates that the model fit reasonably well on the data. Pure error is the standard deviation of replicates at the center points. From model summary in Figure 4.2 it can be seen that the R-sq value, R-sq(adj) And R-sq(pred) values are 96.3%, 95% and 92.6% which are satisfactory. S value represents the standard deviation of the residuals. From the Anova analysis it can be seen that depth of cut is a non-significant factor. So that it has no effect on delamination. But the square terms of cutting speed and depth of cut shows significance on delamination. As depth of cut has no significance on delamination, it's square term can be omitted from the model. Pareto chart of the effect and residual plots are presented in Figure 4.3 below.

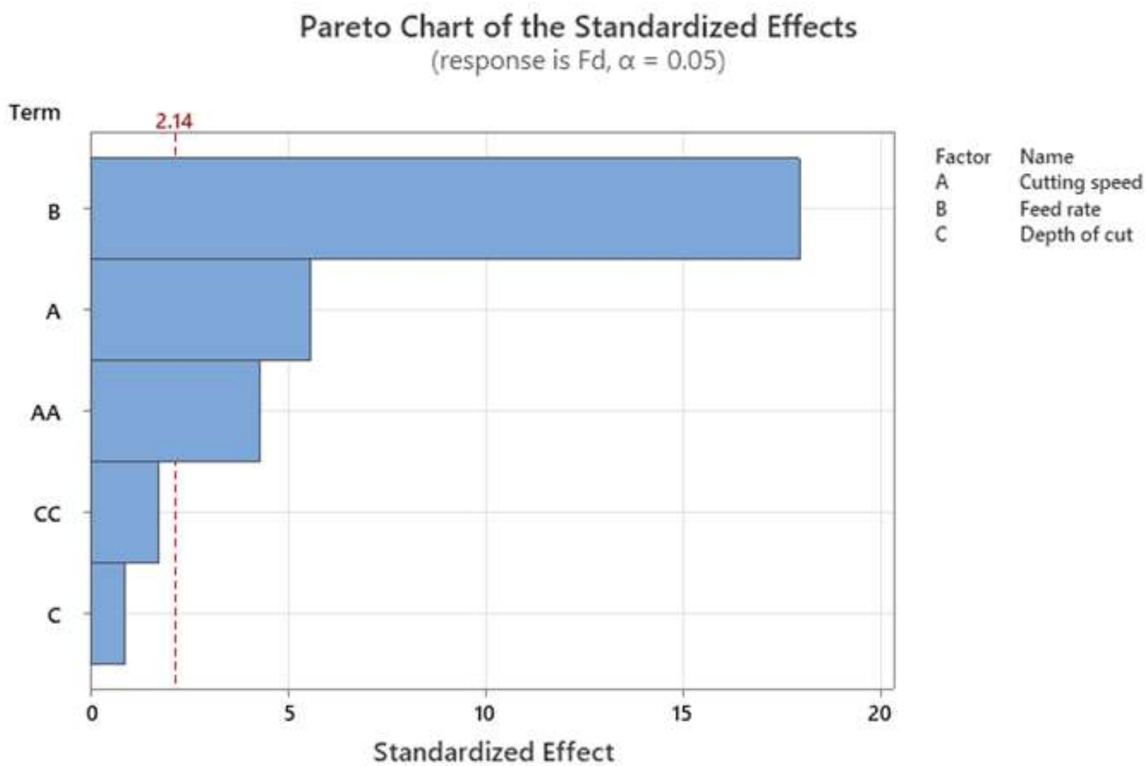

(a)

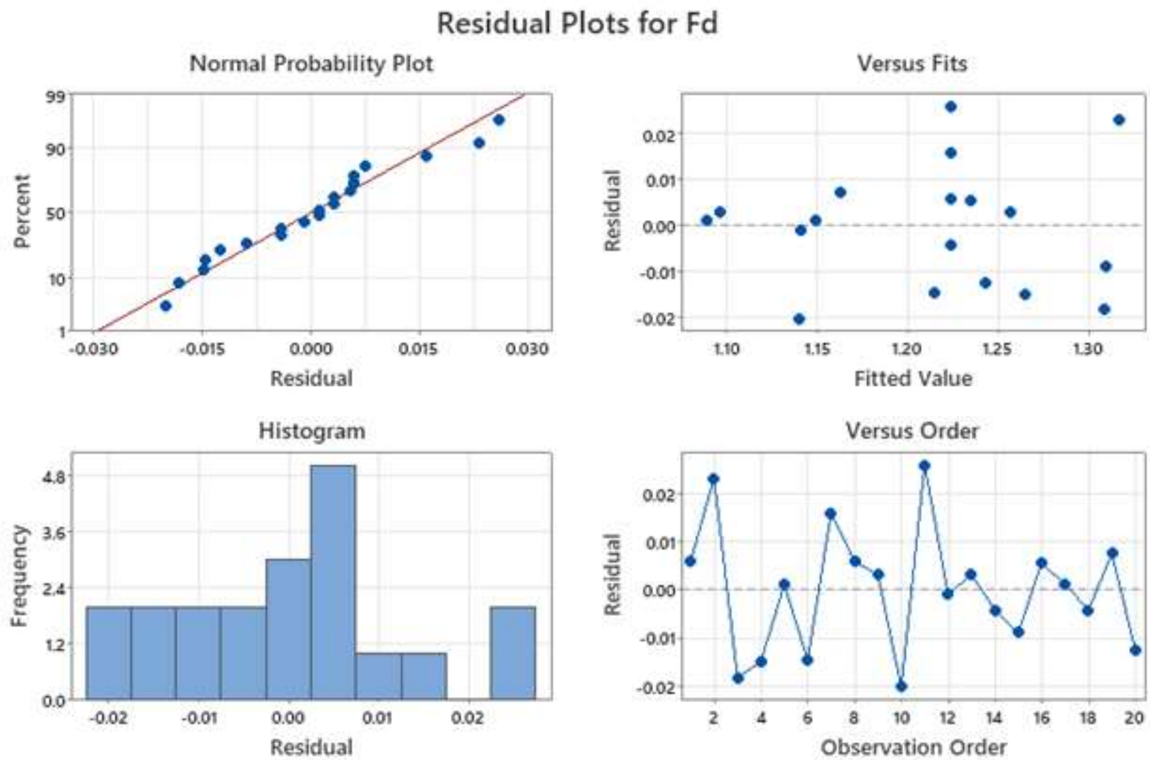

(b)

Figure 4.3: (a) Pareto chart, and (b) residual plots for F_d of the standardized effects.

Regression Equation in Uncoded Units:

F_d = 1.0490 + 0.000116*Cutting speed + 0.001527*Feed rate – 0.0903*Depth of cut – 0.000000*Cutting speed + 0.01438*Depth of cut

Figure 4.4 represents the main effect plots and contour plot for delamination factor.

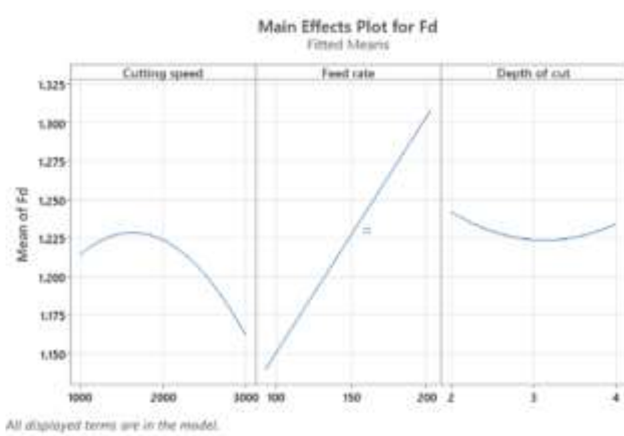

(a)

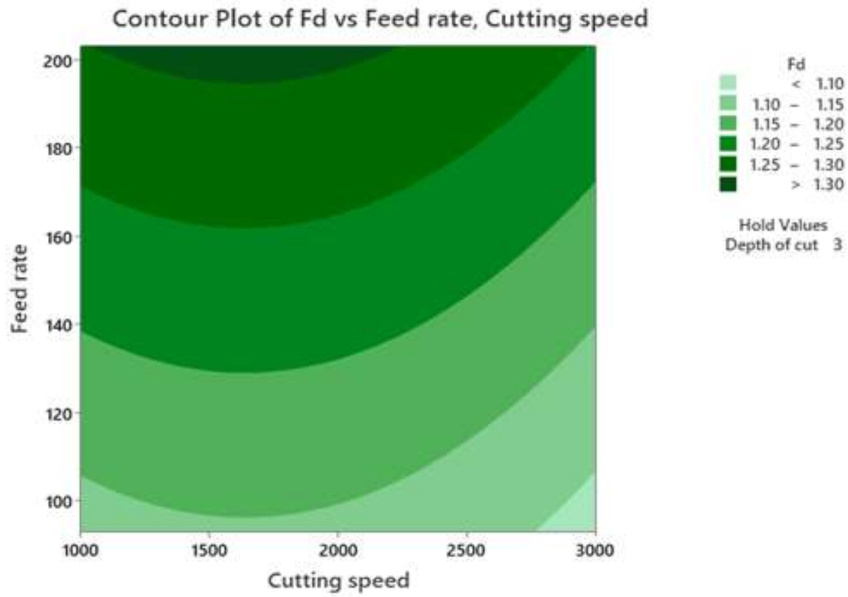

(b)

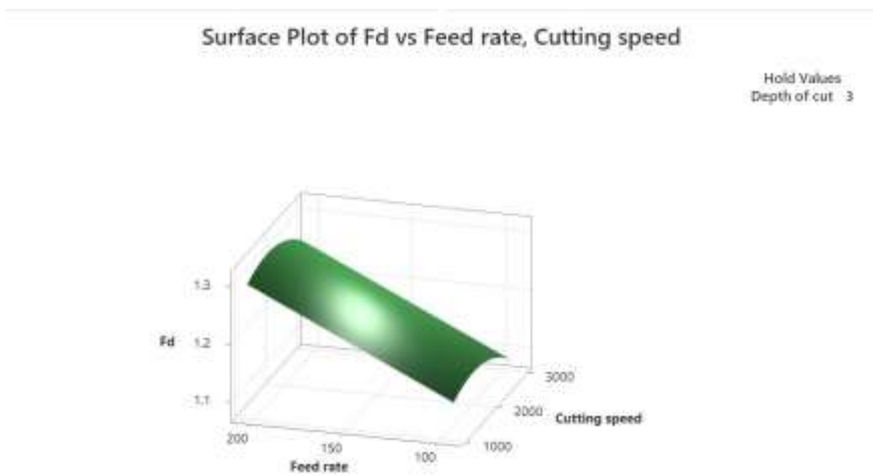

(c)

Figure 4.4: (a) Main effect plots, (b) Contour plot, and (c) Surface plot for delamination factor

It can be deducted that the effect of cutting speed and depth of cut is not linear on delamination. By using the contour plot, amount of delamination can be predicted at any cutting speed and feed rate within the range.

4.3.2 Optimized Response for Minimum Delamination

Parameters

Response	Goal	Lower	Target	Upper	Weight	Importance
Fd	Minimum		1.09	1.34	1	1

Multiple Response Prediction

Variable	Setting
Cutting speed	3000
Feed rate	93
Depth of cut	3.13131

Response	Fit	SE Fit	95% CI	95% PI
Fd	1.0782	0.0104	(1.0559, 1.1005)	(1.0394, 1.1170)

Solutions

Table 4.3: Optimized responses for minimum delamination

Solution	Cutting speed	Feed rate	Depth of cut	Fd Fit	Composite Desirability
1	3000	93	3.13131	1.07822	1.00000
2	3000	93	2.21224	1.09057	0.99771
3	1000	93	3.75746	1.13572	0.81713

4.3.3 Surface Roughness

Table 4.4 presents the results of machining for surface roughness (R_a) using screening parameters for Al_2O_3 nanofiller. All the test runs are provided by the design of experiments by using response surface methodology.

Table 4.4: Surface roughness (R_a) of hybrid composite using Al_2O_3 nanofiller

StdOrder	RunOrder	PtType	Blocks	Cutting speed	Feed rate	Depth of cut	Ra(Al oxide)
1	5	1	1	1000	93	2	8.0
2	13	1	1	3000	93	2	6.9
3	2	1	1	1000	203	2	10.7
4	4	1	1	3000	203	2	9.3
5	12	1	1	1000	93	4	7.9
6	17	1	1	3000	93	4	6.5
7	15	1	1	1000	203	4	10.5
8	9	1	1	3000	203	4	10.2
9	6	-1	1	1000	148	3	9.2
10	19	-1	1	3000	148	3	9.0
11	10	-1	1	2000	93	3	7.5
12	3	-1	1	2000	203	3	9.9
13	20	-1	1	2000	148	2	9.9
14	16	-1	1	2000	148	4	9.5
15	8	0	1	2000	148	3	9.3
16	18	0	1	2000	148	3	9.7
17	1	0	1	2000	148	3	9.6
18	11	0	1	2000	148	3	9.0
19	7	0	1	2000	148	3	9.1
20	14	0	1	2000	148	3	9.2

Anova analysis of the data recorded for surface roughness measurement is represented in Table 4.5

Table 4.5: Anova analysis of surface roughness (Al_2O_3 nanofiller)

Coded Coefficients

Term	Coef	SE Coef	T-Value	P-Value	VIF
Constant	9.350	0.110	85.24	0.000	
Cutting speed	-0.440	0.110	-4.01	0.001	1.00
Feed rate	1.380	0.110	12.58	0.000	1.00
Depth of cut	-0.020	0.110	-0.18	0.858	1.00
Feed rate*Feed rate	-0.610	0.155	-3.93	0.001	1.00

Model Summary

S	R-sq	R-sq(adj)	R-sq(pred)
0.346891	92.68%	90.72%	85.75%

Analysis of Variance

Source	DF	Adj SS	Adj MS	F-Value	P-Value
Model	4	22.8445	5.7111	47.46	0.000
Linear	3	20.9840	6.9947	58.13	0.000
Cutting speed	1	1.9360	1.9360	16.09	0.001
Feed rate	1	19.0440	19.0440	158.26	0.000
Depth of cut	1	0.0040	0.0040	0.03	0.858
Square	1	1.8605	1.8605	15.46	0.001
Feed rate*Feed rate	1	1.8605	1.8605	15.46	0.001
Error	15	1.8050	0.1203		
Lack-of-Fit	10	1.4167	0.1417	1.82	0.263
Pure Error	5	0.3883	0.0777		
Total	19	24.6495			

Regression Equation in Uncoded Units:

R_a (Al_2O_3) = 2.16 - 0.000440*Cutting speed + 0.0848*Feed rate – 0.020*Depth of cut – 0.000202 *Feed rate

The experiment is done considering 95% confidence level. That indicates any P value less than 0.05 indicates that factor is significant. From Table 4.5 it can be deducted that both cutting speed and feed rate are significant which has most effect on roughness. Lack of fit 0.263 indicates that the model fit reasonably well on the data. Pure error is the standard deviation of replicates at the center points. From model summary in Table 4.5 it can be seen that the R-sq value, R-sq(adj) And R-sq(pred) values are 92.68%, 90.72% and 85.75% which are satisfactory and indicates that the analysis model predicts and support the data reasonably. S value represents the standard deviation of the residuals. From the Anova analysis it can be seen that depth of cut is a non-significant factor. So that it has no effect on surface roughness. But the square term of feed rate shows significance on surface roughness. As depth of cut has no significance on delamination, it's square term can be omitted from the model. Pareto chart of the effect and residual plots are presented in Figure 4.5 below

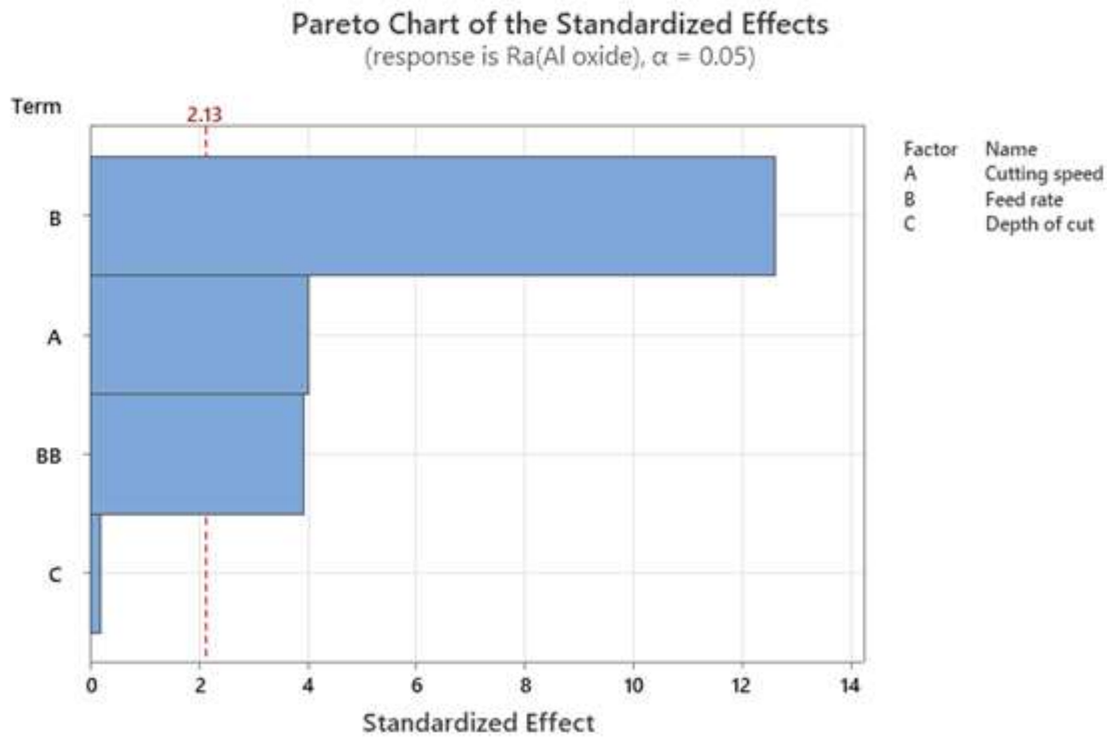

(a)

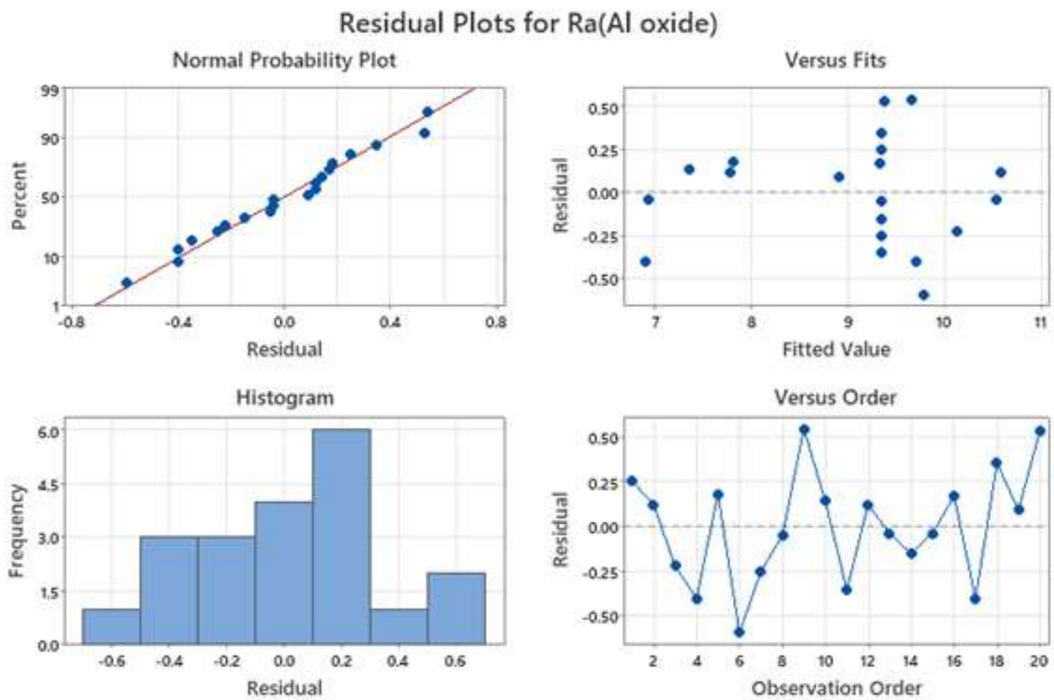

(b)

Figure 4.5: (a) Pareto chart, and (b) residual plots for R_a of the standardized effects.

Figure 4.6 represents the main effect plots for R_a factor. It can be deducted that the effect of cutting speed and depth of cut has linear effect on $R_{a.}$ But the effect of feed rate on surface roughness is non-linear. By using the contour plot, amount of delamination can be predicted at any cutting speed and feed rate within the range.

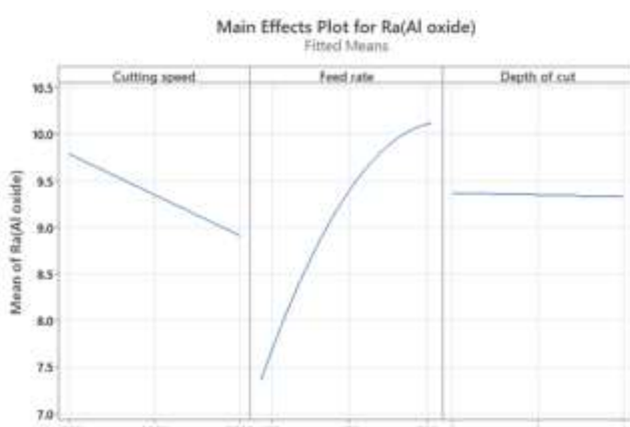

(a)

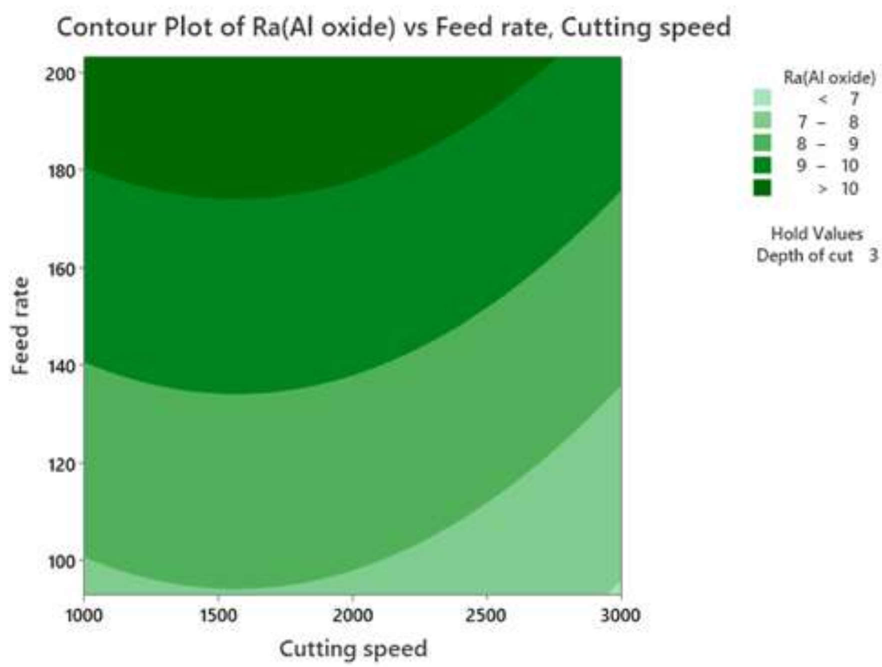

(b)

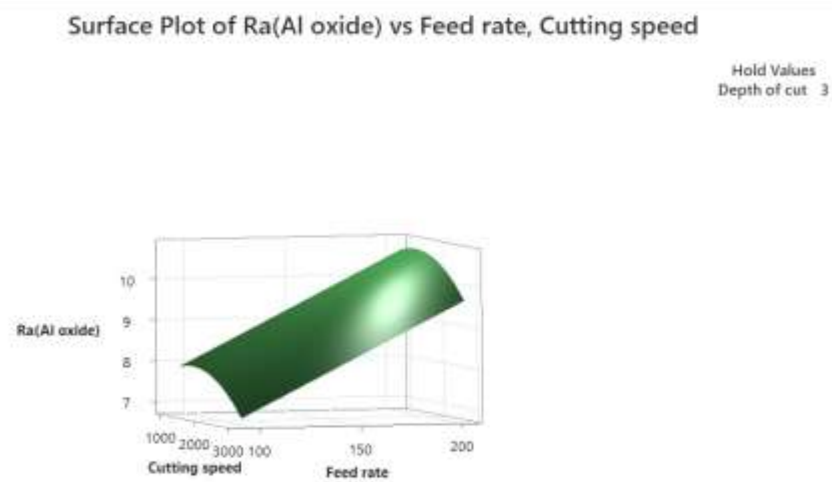

(c)

Figure 4.6: (a) Main effect plot, (b) Contour plot, (c) Surface Plot for roughness factor

4.3.4 Optimized Response for Minimum Surface Roughness

Response	Goal	Lower	Target	Upper	Weight	Importance
Ra	Minimum		6.5	10.7	1	1

Multiple Response Prediction

Variable	Setting
Cutting speed	3000
Feed rate	93
Depth of cut	3.11111

Response	Fit	SE Fit	95% CI	95% PI
Ra(Al oxide)	6.924	0.305	(6.270, 7.577)	(5.788, 8.059)

Table 4.6: Optimized responses (Al_2O_3 nanofiller)

Solution	Cutting speed	Feed rate	Depth of cut	Ra Fit	Composite Desirability
1	3000	93	3.11111	6.92394	0.899063
2	3000	93	3.97933	6.99533	0.882065
3	3000	93	2.02755	7.03310	0.873071

4.4 MACHINING ANALYSIS OF HYBRID COMPOSITE WITH ZnO NANOFILLER

4.4.1 Delamination

Table 4.7 presents the results of machining for delamination using screening parameters. All the test runs are provided by the design of experiments by using response surface methodology.

Table 4.7: Result of delamination (F_d) of hybrid composite using ZnO nanofillers.

StdOrder	RunOrder	PtType	Blocks	Cutting speed	Feed rate	Depth of cut	Ra(Zn oxide)	Fd
1	5	1	1	1000	93	2	3.20	1.13
2	13	1	1	3000	93	2	2.50	1.08
3	2	1	1	1000	203	2	5.40	1.29
4	4	1	1	3000	203	2	4.40	1.24
5	12	1	1	1000	93	4	3.00	1.12
6	17	1	1	3000	93	4	1.80	1.07
7	15	1	1	1000	203	4	5.50	1.27
8	9	1	1	3000	203	4	4.90	1.24
9	6	-1	1	1000	148	3	4.70	1.19
10	19	-1	1	3000	148	3	4.00	1.15
11	10	-1	1	2000	93	3	2.50	1.12
12	3	-1	1	2000	203	3	4.80	1.28
13	20	-1	1	2000	148	2	4.50	1.21
14	16	-1	1	2000	148	4	4.20	1.22
15	8	0	1	2000	148	3	4.30	1.21
16	18	0	1	2000	148	3	4.50	1.20
17	1	0	1	2000	148	3	4.20	1.21
18	11	0	1	2000	148	3	4.44	1.22
19	7	0	1	2000	148	3	4.56	1.22
20	14	0	1	2000	148	3	4.35	1.22

Table 4.8: Anova analysis of delamination (ZnO nanofiller)

Coded Coefficients

Term	Coef	SE Coef	T-Value	P-Value	VIF
Constant	1.21100	0.00276	438.04	0.000	
Cutting speed	-0.02200	0.00276	-7.96	0.000	1.00
Feed rate	0.08000	0.00276	28.94	0.000	1.00
Depth of cut	-0.00300	0.00276	-1.09	0.296	1.00
Cutting speed*Cutting speed	-0.03300	0.00391	-8.44	0.000	1.00
Cutting speed*Feed rate	0.00250	0.00309	0.81	0.432	1.00

Model Summary

S	R-sq	R-sq(adj)	R-sq(pred)
0.0087423	98.58%	98.08%	97.31%

Analysis of Variance

Source	DF	Adj SS	Adj MS	F-Value	P-Value
Model	5	0.074425	0.014885	194.76	0.000
Linear	3	0.068930	0.022977	300.63	0.000
Cutting speed	1	0.004840	0.004840	63.33	0.000
Feed rate	1	0.064000	0.064000	837.38	0.000
Depth of cut	1	0.000090	0.000090	1.18	0.296
Square	1	0.005445	0.005445	71.24	0.000
Cutting speed*Cutting speed	1	0.005445	0.005445	71.24	0.000
2-Way Interaction	1	0.000050	0.000050	0.65	0.432
Cutting speed*Feed rate	1	0.000050	0.000050	0.65	0.432
Error	14	0.001070	0.000076		
Lack-of-Fit	9	0.000737	0.000082	1.23	0.432
Pure Error	5	0.000333	0.000067		
Total	19	0.075495			

Regression Equation in Uncoded Units (ZnO nanofiller):

F_d = 0.9302 + 0.000103*Cutting speed + 0.001364*Feed rate – 0.00300*Depth of cut – 0.000000*Cutting speed + 0.0000000* Cutting speed*Feed rate

The experiment is done considering 95% confidence level. That indicates any P value less than 0.05 indicates that factor is significant. From the gathered information from Table 4.8 it can be deducted that both cutting speed and feed rate are significant which has most effect on delamination. Lack of fit 0.432 indicates that the model fit reasonably well on the data. Pure error is the standard deviation of replicates at the center points. From model summary, it can be seen that the R-sq value, R-sq(adj) And R-sq(pred) values are 98%, 98% and 97% which are satisfactory. S value represents the standard deviation of the residuals. From the Anova analysis it can be seen that depth of cut is a non-significant factor. So that it has no effect on delamination. But the square terms of cutting speed shows significance on delamination. As depth of cut has no significance on delamination, it's square term can be omitted from the model. Pareto chart of the effect and residual plots are presented in Figure 4.7 below.

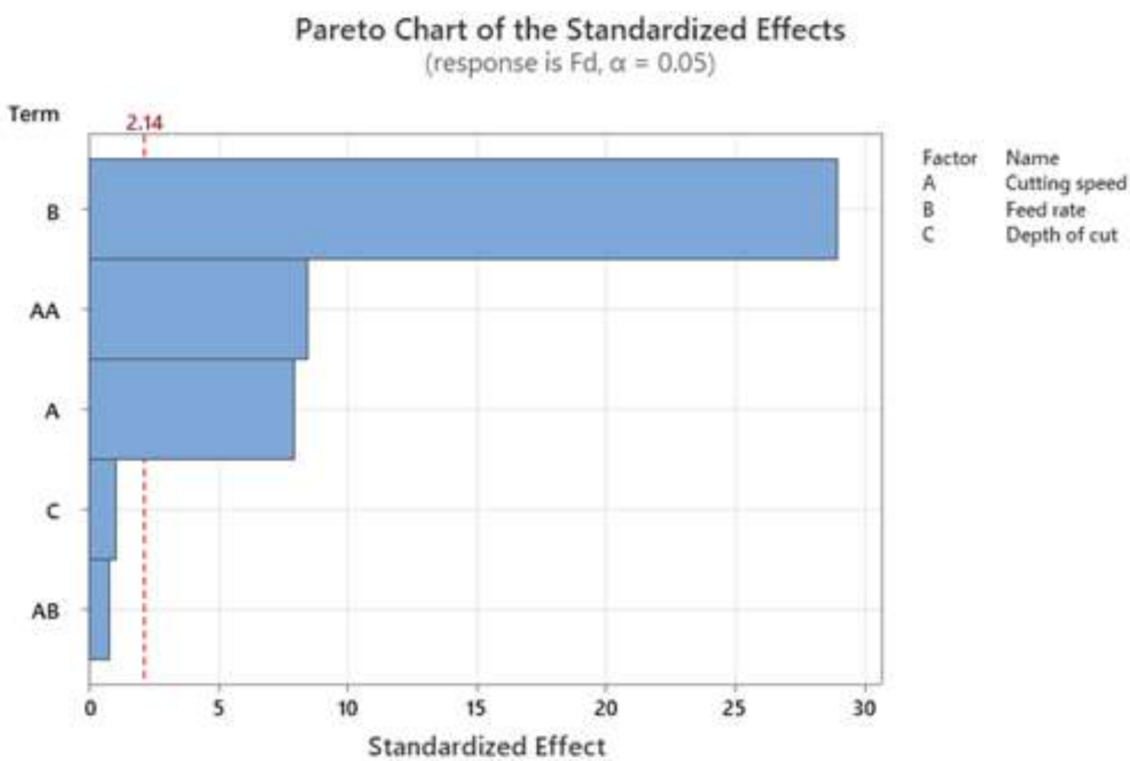

(a)

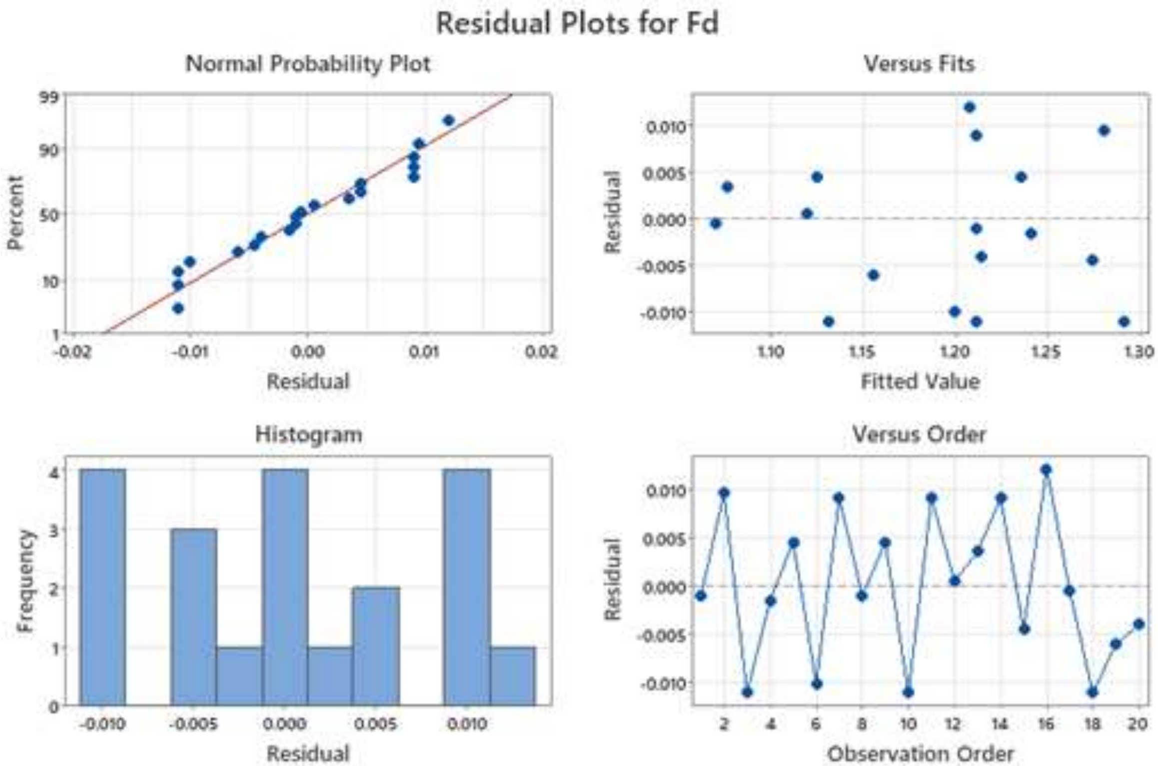

(b)

Figure 4.7: (a) Pareto chart, and (b) Residual plots for F_d of the standardized effects

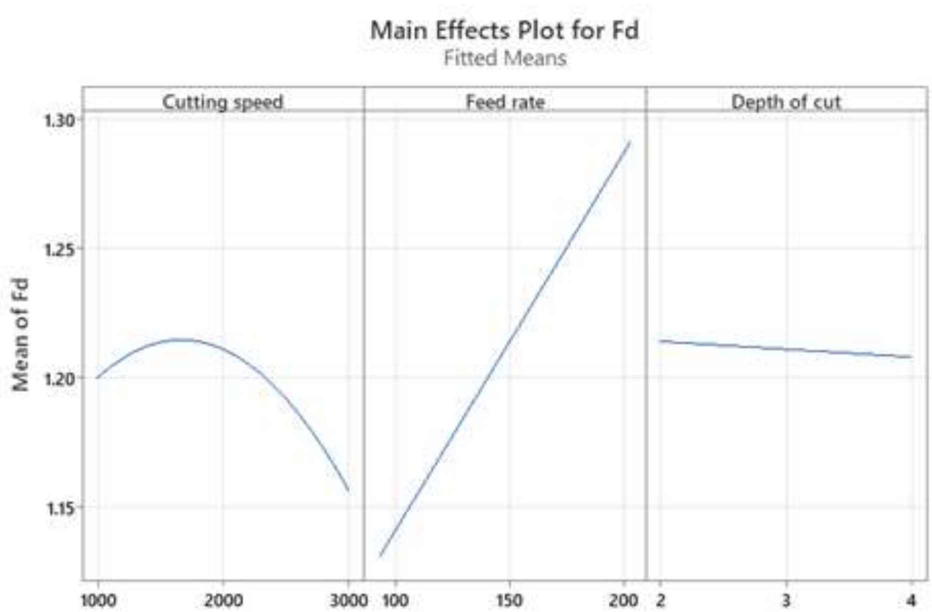

(a)

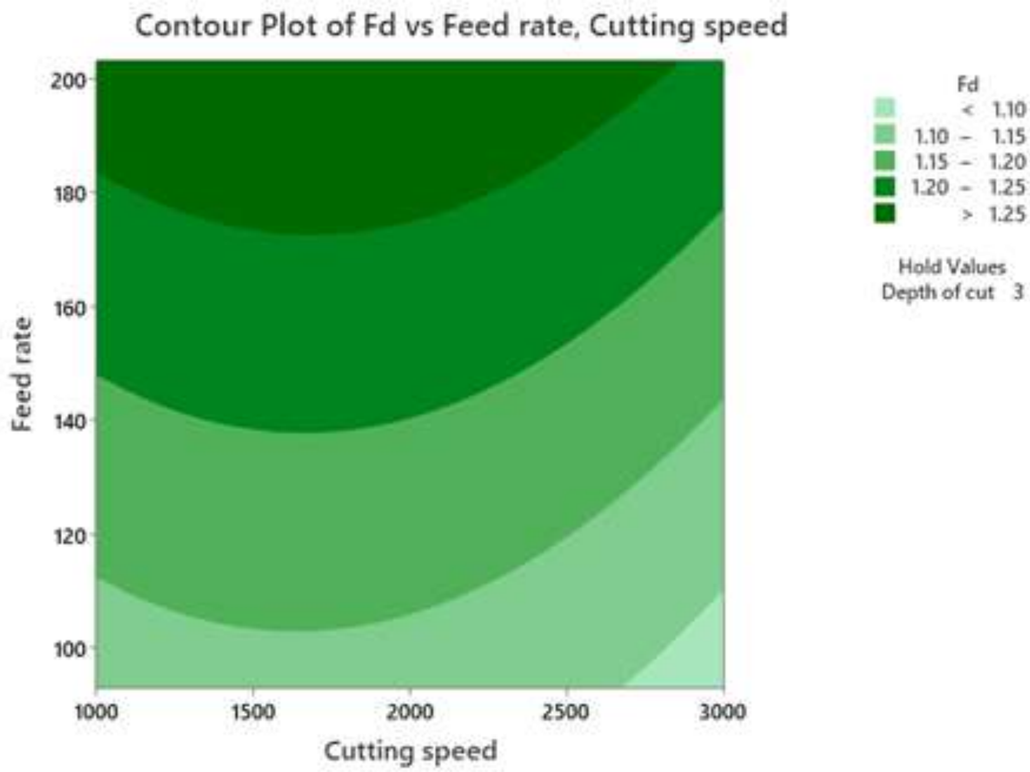

(b)

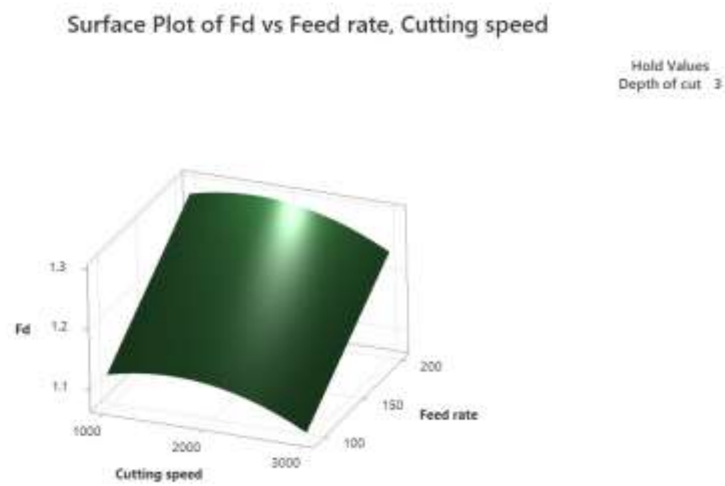

(c)

Figure 4.8: (a) Main effect plot, (b) Contour plot, and (c) Surface plot for F_d (ZnO nanofiller)

4.4.2 Optimized Response for Minimum Delamination

Table 4.9: Optimized responses for F_d

Multiple Response Prediction

Variable	Setting
Cutting speed	3000
Feed rate	93
Depth of cut	4

Response	Fit	SE Fit	95% CI	95% PI
Fd	1.07050	0.00633	(1.05691, 1.08409)	(1.04734, 1.09366)

Solutions

Solution	Cutting speed	Feed rate	Depth of cut	Fd Fit	Composite Desirability
1	3000	93	4.00000	1.07050	0.997727
2	3000	93	2.00130	1.07650	0.970472

4.4.3 Surface Roughness

From Table 4.10 it can be deducted that both cutting speed and feed rate are significant which has most effect on R_a. Lack of fit 0.468 indicates that the model fit reasonably well on the data. Pure error is the standard deviation of replicates at the center points. From model summary in Table 4.10 it can be seen that the R-sq value, R-sq(adj) And R-sq(pred) values are 98%, 97% and 96% which are satisfactory. S value represents the standard deviation of the residuals. From the anova analysis it can be seen that depth of cut is a non-significant factor. So that it has no effect on roughness. But the square terms of feed rate show significance on $R_{a.}$ Also 2-way interaction of feed rate and depth of cut has significance on delamination, this could happen because of layer-by-layer structure of the composite and can be considered as an error due to machining. Pareto chart of the effect and residual plots are presented in Figure 4.9 below.

Table 4.10: Anova analysis of R_a (ZnO nanofiller)

Coded Coefficients

Term	Coef	SE Coef	T-Value	P-Value	VIF
Constant	4.3750	0.0441	99.22	0.000	
Cutting speed	-0.3800	0.0441	-8.62	0.000	1.00
Feed rate	1.1600	0.0441	26.31	0.000	1.00
Depth of cut	-0.0200	0.0441	-0.45	0.657	1.00
Feed rate*Feed rate	-0.5350	0.0624	-8.58	0.000	1.00
Feed rate*Depth of cut	0.1375	0.0493	2.79	0.014	1.00

Model Summary

S	R-sq	R-sq(adj)	R-sq(pred)
0.139438	98.38%	97.80%	96.43%

Analysis of Variance

Source	DF	Adj SS	Adj MS	F-Value	P-Value
Model	5	16.4864	3.2973	169.59	0.000
Linear	3	14.9040	4.9680	255.52	0.000
Cutting speed	1	1.4440	1.4440	74.27	0.000
Feed rate	1	13.4560	13.4560	692.08	0.000
Depth of cut	1	0.0040	0.0040	0.21	0.657
Square	1	1.4311	1.4311	73.61	0.000
Feed rate*Feed rate	1	1.4311	1.4311	73.61	0.000
2-Way Interaction	1	0.1512	0.1512	7.78	0.014
Feed rate*Depth of cut	1	0.1512	0.1512	7.78	0.014
Error	14	0.2722	0.0194		
Lack-of-Fit	9	0.1829	0.0203	1.14	0.468
Pure Error	5	0.0893	0.0179		
Total	19	16.7586			

Regression Equation in Uncoded Units

R_a (ZnO) = - 0.690 - 0.000380 Cutting speed + 0.06594 Feed rate - 0.390 Depth of cut - 0.000177 Feed rate*Feed rate + 0.002500 Feed rate*Depth of cut

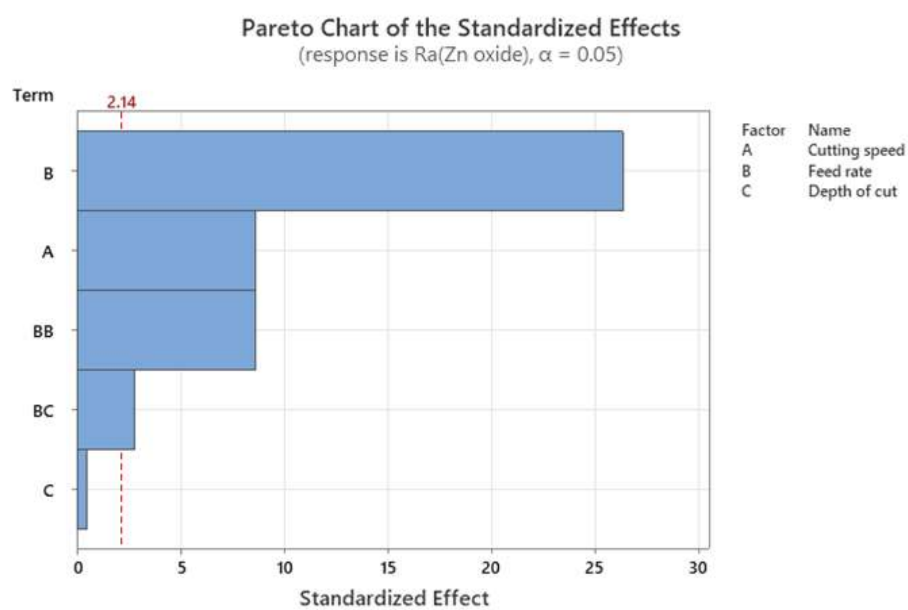

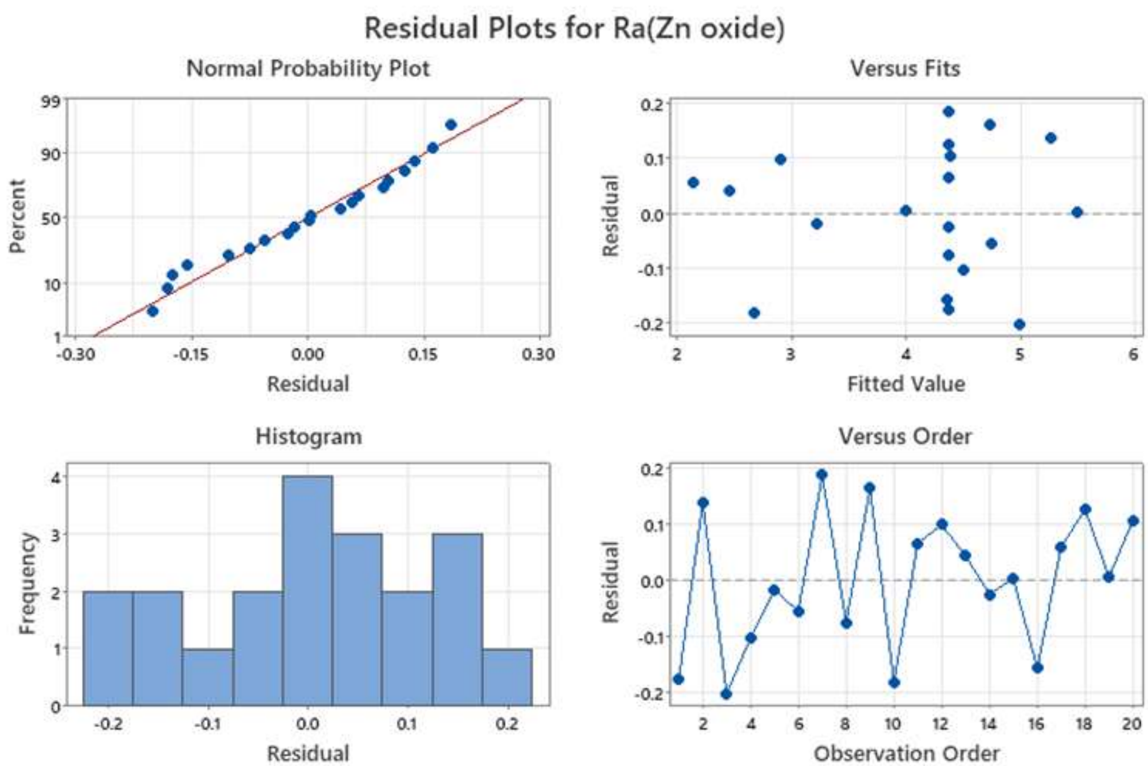

Figure 4.9: (a) Pareto chart, and (b) Residual plots for R_a of the standardized effects (ZnO nanofiller)

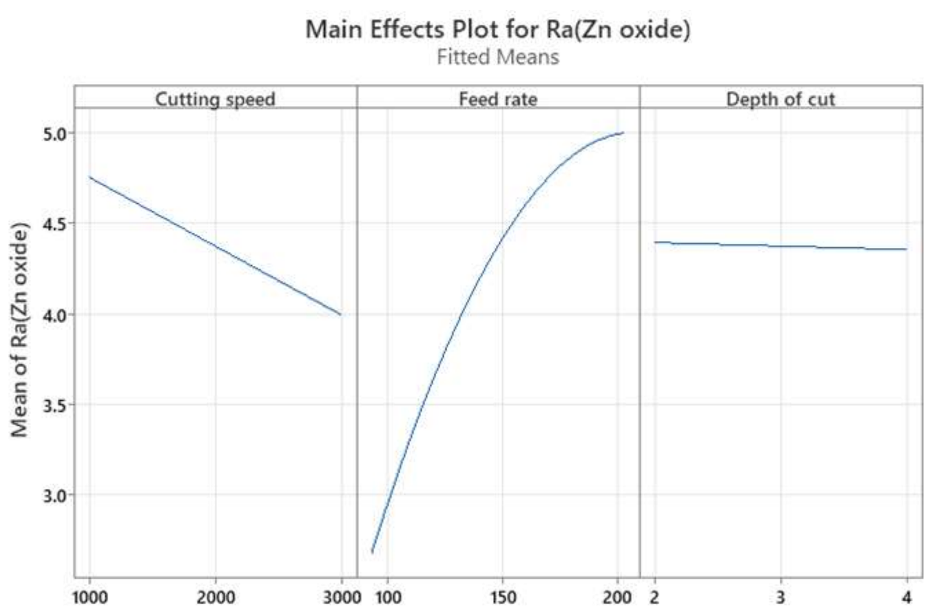

(a)

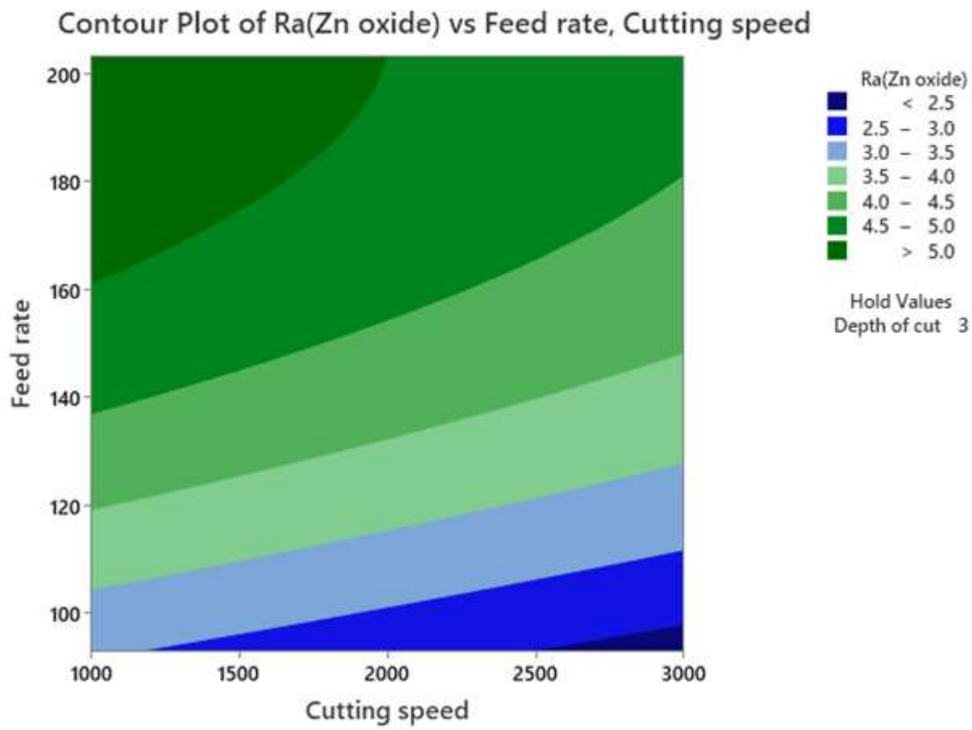
Contour Plot of Ra(Zn oxide) vs Feed rate, Cutting speed
Feed rate
200
180
160
140
120
100
1000
1500
2000
2500
3000
Cutting speed
Ra(Zn oxide)
< 2.5
2.5 – 3.0
3.0 – 3.5
3.5 – 4.0
4.0 – 4.5
4.5 – 5.0
> 5.0
Hold Values
Depth of cut 3

(b)

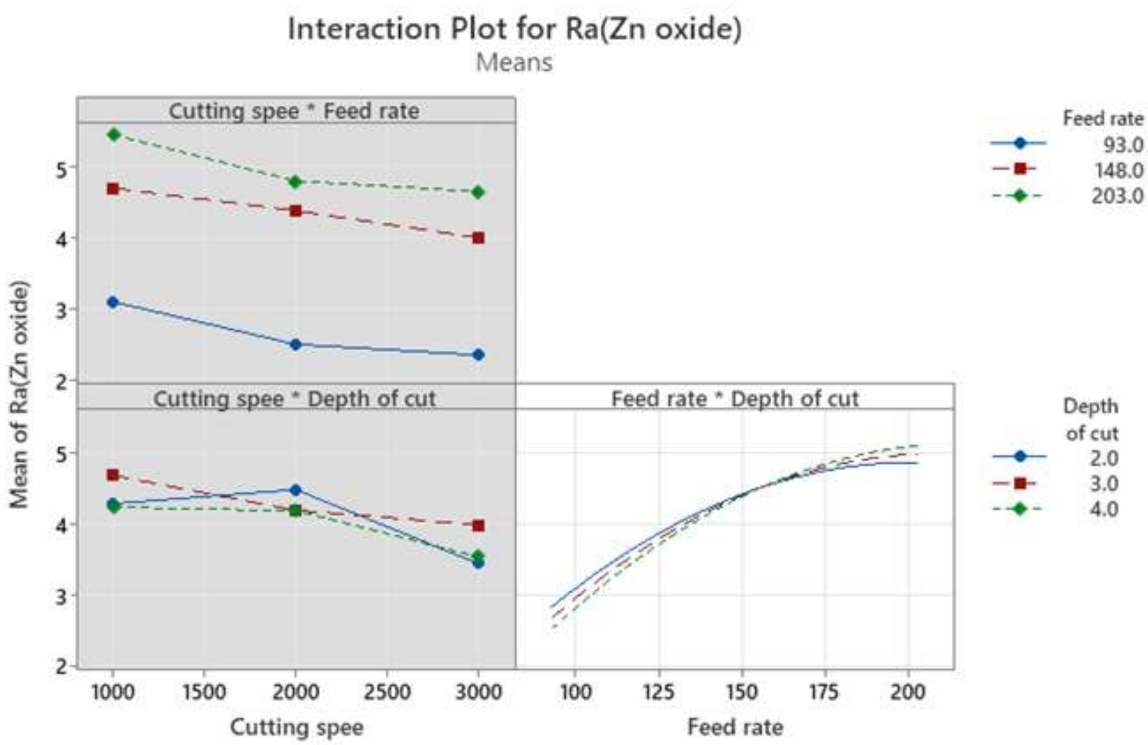
Interaction Plot for Ra(Zn oxide)
Means
Cutting spee * Feed rate
Cutting spee * Depth of cut
Feed rate * Depth of cut
Mean of Ra(Zn oxide)
5
4
3
2
1000
1500
2000
2500
3000
Cutting spee
100
125
150
175
200
Feed rate
Feed rate
93.0
148.0
203.0
Depth of cut
2.0
3.0
4.0

(c)

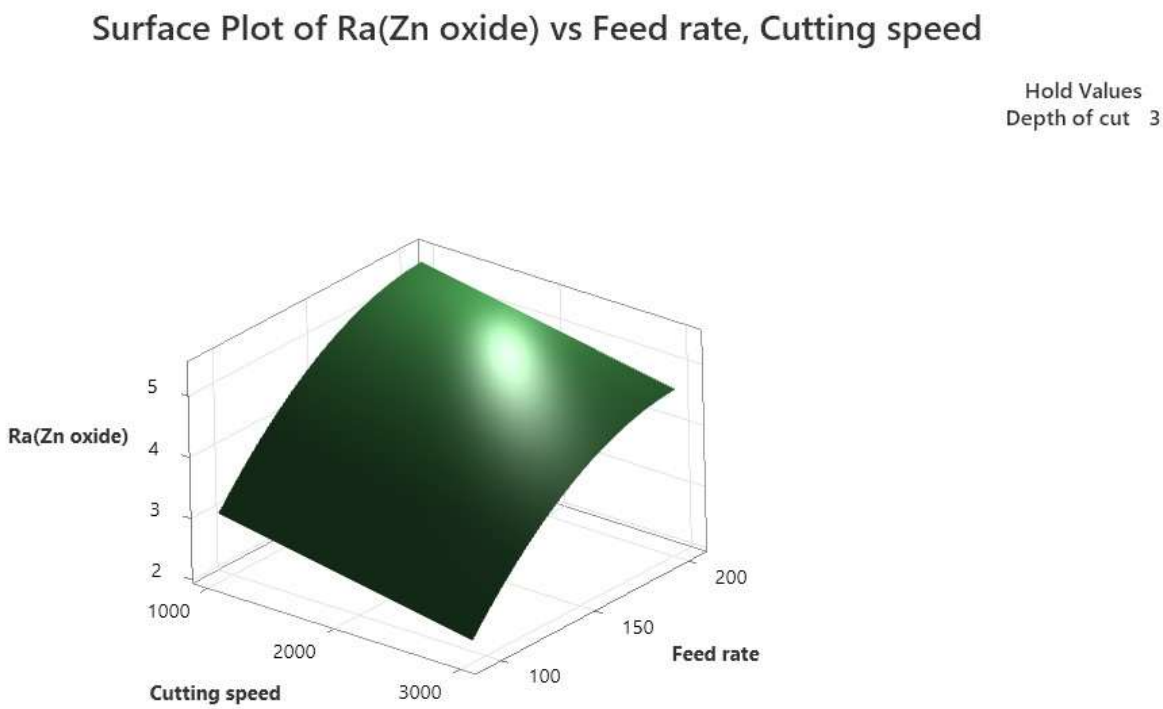

(d)

Figure 4.10: (a) Main effect plot, (b) contour plot, (c) Interaction plot, and (d) Surface plot for R_a (ZnO)

4.4.4 Optimized Response for Minimum Surface Roughness

Table 4.11: Optimized responses for R_a (ZnO)

Parameters

Response	Goal	Lower	Target	Upper	Weight	Importance
Ra(Zn oxide)	Minimum		2.2	5.5	1	1

Solutions

Solution	Cutting speed	Feed rate	Depth of cut	Ra(Zn oxide) Fit	Composite Desirability
1	3000	93	4.00000	2.1425	1
2	3000	93	3.63492	2.2000	1

Multiple Response Prediction

Variable	Setting
Cutting speed	3000
Feed rate	93
Depth of cut	4

Response	Fit	SE Fit	95% CI	95% PI
Ra(Zn oxide)	2.143	0.101	(1.926, 2.359)	(1.773, 2.512)

4.5 MACHINING ANALYSIS HYBRID COMPOSITE WITH TiO_2 NANOFILLER

4.5.1 Delamination

Table 4.12 presents the results of machining for surface roughness (R_a) and delamination (F_d) using screening parameters. All the test runs are provided by the design of experiments by using response surface methodology.

Table 4.12: Result of delamination (F_d) of hybrid composite using TiO_2 nanofillers.

StdOrder	RunOrder	PtType	Blocks	Cutting speed	Feed rate	Depth of cut	Fd
1	5	1	1	1000	93	2	1.12
2	13	1	1	3000	93	2	1.08
3	2	1	1	1000	203	2	1.30
4	4	1	1	3000	203	2	1.24
5	12	1	1	1000	93	4	1.13
6	17	1	1	3000	93	4	1.07
7	15	1	1	1000	203	4	1.27
8	9	1	1	3000	203	4	1.23
9	6	-1	1	1000	148	3	1.18
10	19	-1	1	3000	148	3	1.12
11	10	-1	1	2000	93	3	1.10
12	3	-1	1	2000	203	3	1.25
13	20	-1	1	2000	148	2	1.19
14	16	-1	1	2000	148	4	1.20
15	8	0	1	2000	148	3	1.19
16	18	0	1	2000	148	3	1.20
17	1	0	1	2000	148	3	1.18
18	11	0	1	2000	148	3	1.19
19	7	0	1	2000	148	3	1.20
20	14	0	1	2000	148	3	1.20

Table 4.13: Anova analysis of F_d for TiO_2 nanofiller

Coded Coefficients

Term	Coef	SE Coef	T-Value	P-Value	VIF
Constant	1.18637	0.00394	301.35	0.000	
Cutting speed	-0.02600	0.00371	-7.00	0.000	1.00
Feed rate	0.07900	0.00371	21.28	0.000	1.00
Depth of cut	-0.00300	0.00371	-0.81	0.432	1.00
Cutting speed*Cutting speed	-0.02687	0.00656	-4.10	0.001	1.56
Depth of cut*Depth of cut	0.01812	0.00656	2.76	0.015	1.56

Model Summary

S	R-sq	R-sq(adj)	R-sq(pred)
0.0117375	97.38%	96.44%	94.37%

Analysis of Variance

Source	DF	Adj SS	Adj MS	F-Value	P-Value
Model	5	0.071591	0.014318	103.93	0.000
Linear	3	0.069260	0.023087	167.58	0.000
Cutting speed	1	0.006760	0.006760	49.07	0.000
Feed rate	1	0.062410	0.062410	453.01	0.000
Depth of cut	1	0.000090	0.000090	0.65	0.432
Square	2	0.002331	0.001166	8.46	0.004
Cutting speed*Cutting speed	1	0.002311	0.002311	16.78	0.001
Depth of cut*Depth of cut	1	0.001051	0.001051	7.63	0.015
Error	14	0.001929	0.000138		
Lack-of-Fit	9	0.001595	0.000177	2.66	0.147
Pure Error	5	0.000333	0.000067		
Total	19	0.073520			

Regression Equation in Uncoded Units:

F_d = 1.0904 + 0.000081*Cutting speed + 0.001436*Feed rate – 0.1118*Depth of cut – 0.000000*Cutting speed + 0.01812* Depth of cut

The experiment is done considering 95% confidence level. That indicates any P value less than 0.05 indicates that factor is significant. From Table 4.12 it can be deducted that both cutting speed and feed rate are significant which has most effect on roughness. Lack of fit 0.147 indicates that the model fit reasonably well on the data. Pure error is the standard deviation of replicates at the center points. From model summary in Table 4.13 it can be seen that the R-sq value, R-sq(adj) And R-sq(pred) values are 97%, 90.72% and 94.3% which are satisfactory and indicates that the analysis model predicts and support the data reasonably. S value represents the standard deviation of the residuals. From the anova analysis it can be seen that depth of cut is a non-significant factor. So that it has no effect on surface roughness. But the square term of feed rate shows significance on surface roughness. As depth of cut has no significance on delamination, it's square term can be omitted from the model. Pareto chart of the effect and residual plots are presented in Figure 4.11 below. Main effects are illustrated in Figure 4.12.

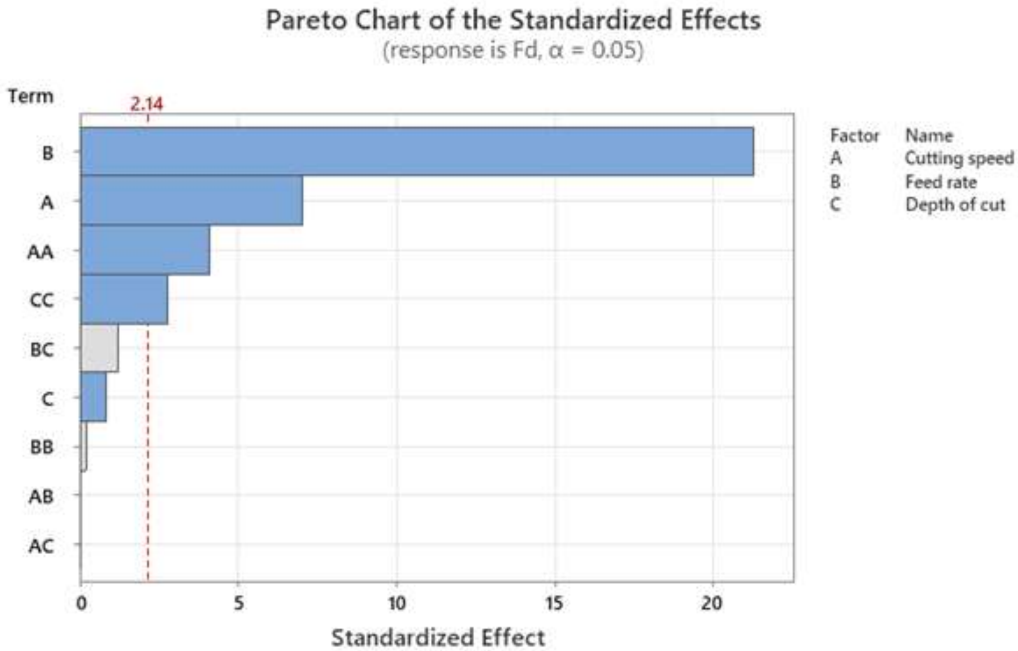

(a)

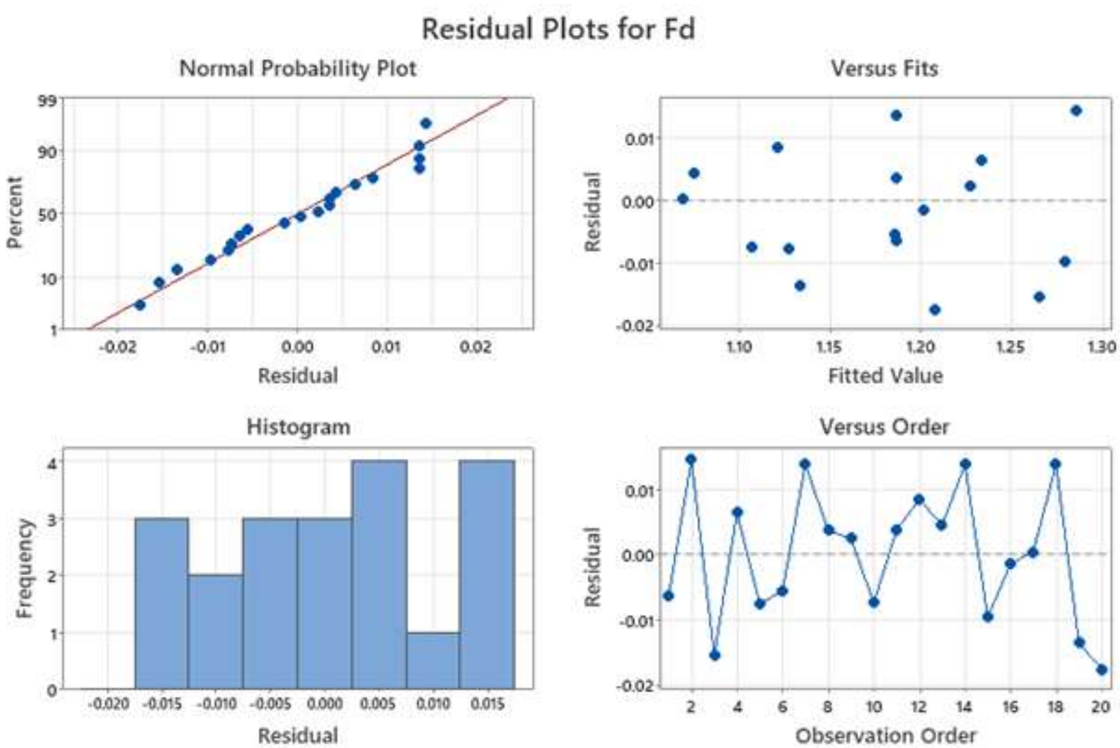

(b)

Figure 4.11: (a) Pareto chart and (b) Residual plots for F_d of the standardized effects (TiO_2)

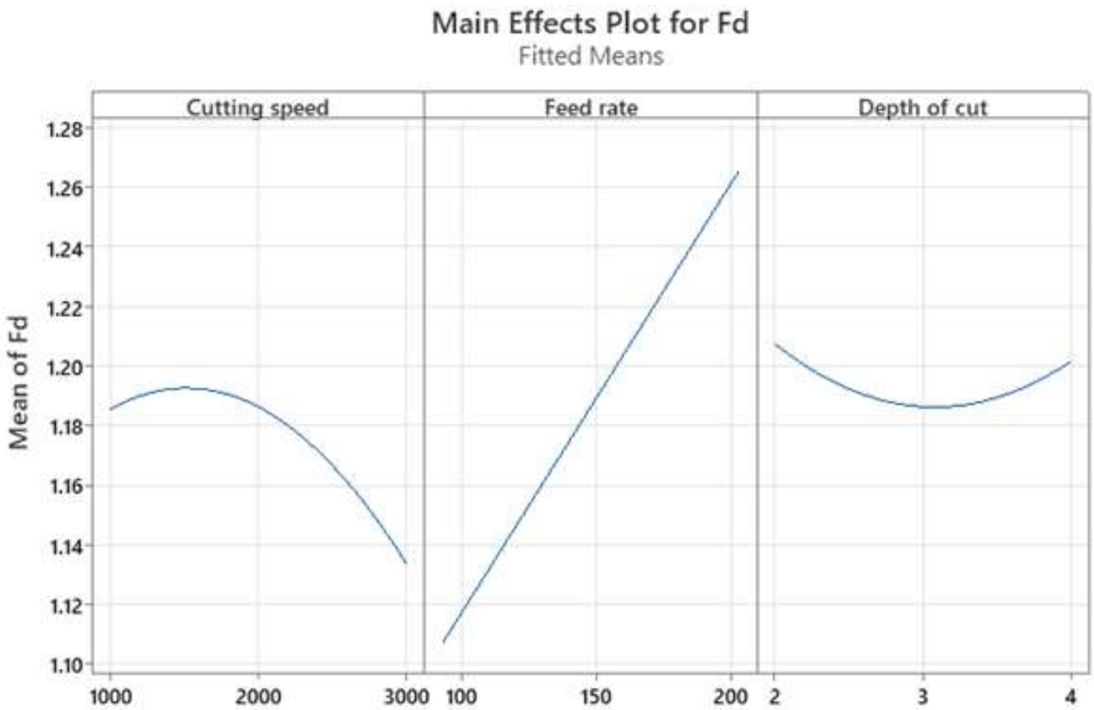

Main Effects Plot for Fd
Fitted Means
Cutting speed
Feed rate
Depth of cut
Mean of Fd
1.28
1.26
1.24
1.22
1.20
1.18
1.16
1.14
1.12
1.10
1000
2000
3000
100
150
200
2
3
4

(a)

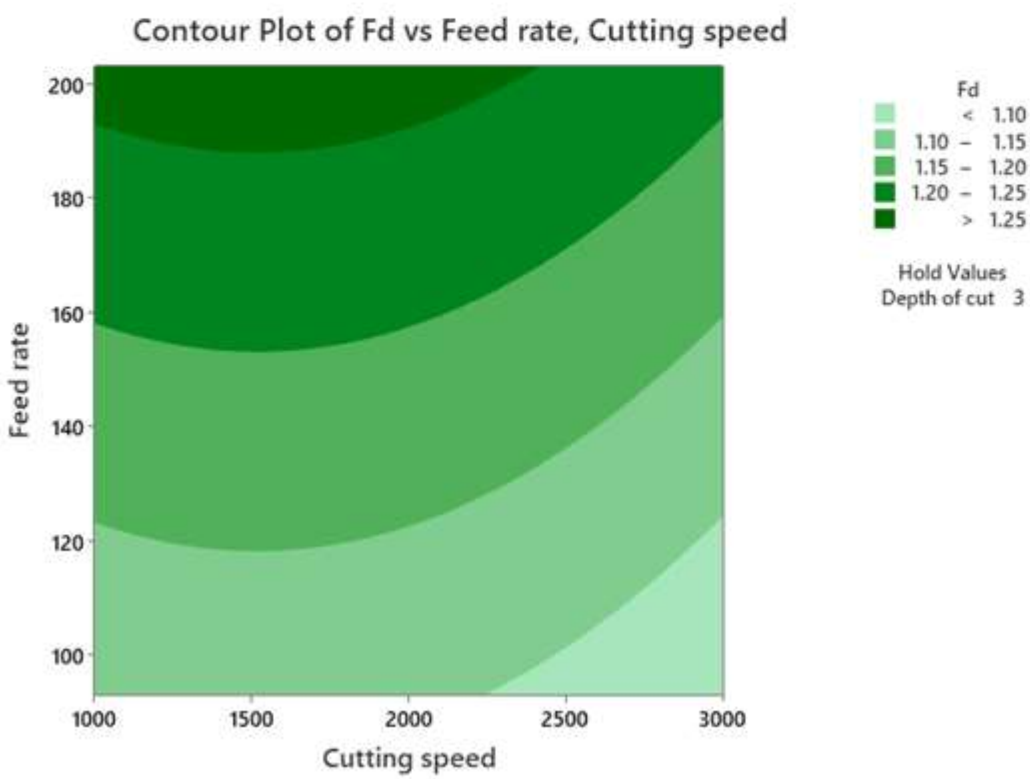

Contour Plot of Fd vs Feed rate, Cutting speed
Feed rate
Cutting speed
200
180
160
140
120
100
1000
1500
2000
2500
3000
Fd
< 1.10
1.10 – 1.15
1.15 – 1.20
1.20 – 1.25
> 1.25
Hold Values
Depth of cut 3

(b)

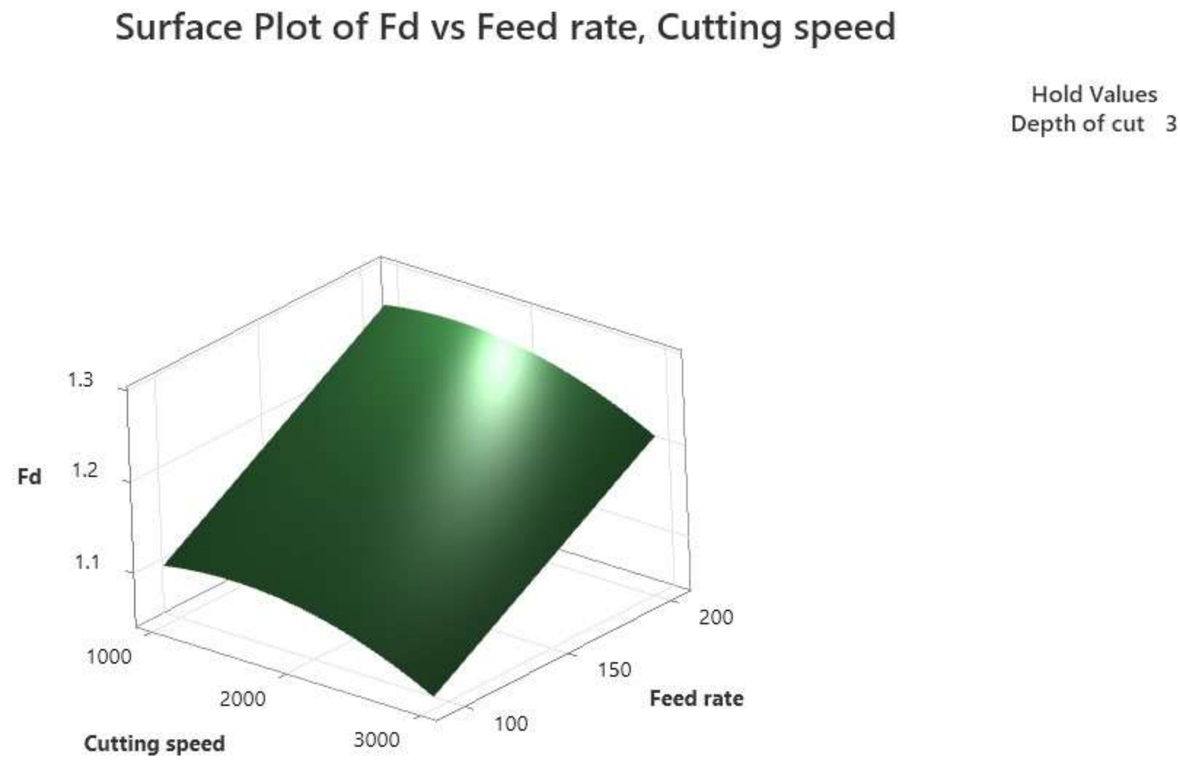

(c)

Figure 4.12: (a) Main effect plot, (b) Contour plot, and (c) Surface plot of F_d (TiO_2)

From the main effect plot in Figure 4.12 it can be seen that in case of TiO_2 as nanofiller, the effect of cutting speed on delamination is not linear. The effect of depth of cut can be ignored as it is not significant according to the pareto chart of standardized effects. Moreover, contour plot is presented, from which delamination at any feed rate and cutting speed can be predicted.

4.5.2 Optimized Response for F_d

Table 4.14: Optimized responses for F_d (TiO_2)

Parameters

Response	Goal	Lower	Target	Upper	Weight	Importance
Fd	Minimum		1.07	1.3	1	1

Solutions

Solution	Cutting speed	Feed rate	Depth of cut	Fd Fit	Composite Desirability
1	3000	93	3.09091	1.05438	1.00000
2	3000	93	2.14529	1.07030	0.99867

Multiple Response Prediction

Variable	Setting
Cutting speed	3000
Feed rate	93
Depth of cut	3.09091

Response	Fit	SE Fit	95% CI	95% PI
Fd	1.05438	0.00827	(1.03663, 1.07212)	(1.02358, 1.08518)

4.5.3 Surface Roughness

Table 4.15: Result of Surface roughness (R_a) of hybrid composite using TiO_2 nanofillers.

StdOrder	RunOrder	PtType	Blocks	Cutting speed	Feed rate	Depth of cut	Ra(Ti oxide)
1	5	1	1	1000	93	2	6.1
2	13	1	1	3000	93	2	4.8
3	2	1	1	1000	203	2	8.3
4	4	1	1	3000	203	2	7.5
5	12	1	1	1000	93	4	6.0
6	17	1	1	3000	93	4	4.7
7	15	1	1	1000	203	4	8.4
8	9	1	1	3000	203	4	8.1
9	6	-1	1	1000	148	3	7.8
10	19	-1	1	3000	148	3	7.0
11	10	-1	1	2000	93	3	5.4
12	3	-1	1	2000	203	3	7.9
13	20	-1	1	2000	148	2	7.4
14	16	-1	1	2000	148	4	7.3
15	8	0	1	2000	148	3	7.3
16	18	0	1	2000	148	3	7.5
17	1	0	1	2000	148	3	7.3
18	11	0	1	2000	148	3	7.2
19	7	0	1	2000	148	3	7.3
20	14	0	1	2000	148	3	7.4

Table 4.16: Anova analysis of R_a (TiO_2)

Coded Coefficients

Term	Coef	SE Coef	T-Value	P-Value	VIF
Constant	7.3500	0.0365	201.19	0.000	
Cutting speed	-0.4500	0.0365	-12.32	0.000	1.00
Feed rate	1.3200	0.0365	36.13	0.000	1.00
Depth of cut	0.0400	0.0365	1.09	0.293	1.00
Feed rate*Feed rate	-0.6300	0.0517	-12.19	0.000	1.00
Cutting speed*Feed rate	0.1875	0.0408	4.59	0.001	1.00
Feed rate*Depth of cut	0.1125	0.0408	2.75	0.016	1.00

Model Summary

S	R-sq	R-sq(adj)	R-sq(pred)
0.115526	99.21%	98.85%	96.67%

Analysis of Variance

Source	DF	Adj SS	Adj MS	F-Value	P-Value
Model	6	21.8320	3.6387	272.64	0.000
Linear	3	19.4650	6.4883	486.16	0.000
Cutting speed	1	2.0250	2.0250	151.73	0.000
Feed rate	1	17.4240	17.4240	1305.54	0.000
Depth of cut	1	0.0160	0.0160	1.20	0.293
Square	1	1.9845	1.9845	148.69	0.000
Feed rate*Feed rate	1	1.9845	1.9845	148.69	0.000
2-Way Interaction	2	0.3825	0.1912	14.33	0.001
Cutting speed*Feed rate	1	0.2812	0.2812	21.07	0.001
Feed rate*Depth of cut	1	0.1012	0.1012	7.59	0.016
Error	13	0.1735	0.0133		
Lack-of-Fit	8	0.1202	0.0150	1.41	0.367
Pure Error	5	0.0533	0.0107		
Total	19	22.0055			

Regression Equation in Uncoded Units:

R_a (TiO_2) = 1.933 - 0.000955*Cutting speed + 0.07269*Feed rate – 0.263*Depth of cut – 0.000208 *Feed rate + 0.000003*Cutting speed*Feed rate + 0.002045*Feed rate*Depth of cut

From Table 4.15 it can be deducted that both cutting speed and feed rate are significant which has most effect on R_a. Lack of fit 0.367 indicates that the model fit reasonably well on the data. Pure error is the standard deviation of replicates at the center points. From model summary in Table 4.16 it can be seen that the R-sq value, R-sq(adj) And R-sq(pred) values are 99%, 98% and 96% which are satisfactory. S value represents the standard deviation of the residuals. From the anova analysis it can be seen that depth of cut is a non-significant factor. So that it has no effect on R_a. But the square terms of feed rate show significance on $R_{a.}$ Also, from the anova analysis, cutting speed and fed rate interaction shows significance on roughness factor. Also 2-way interaction of feed rate and depth of cut has significance on delamination, this could happen because of layer-by-layer structure of the composite and can be considered as an error due to machining. Pareto chart of the effect, residual plots and interaction plots are presented in Figure 4.13 below.

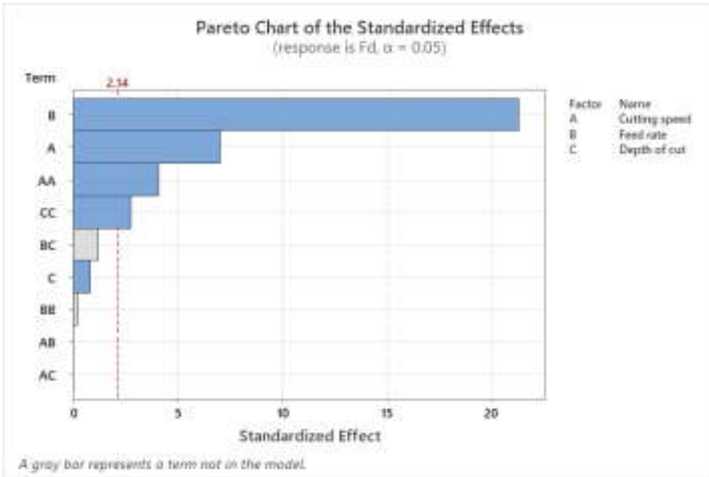

(a)

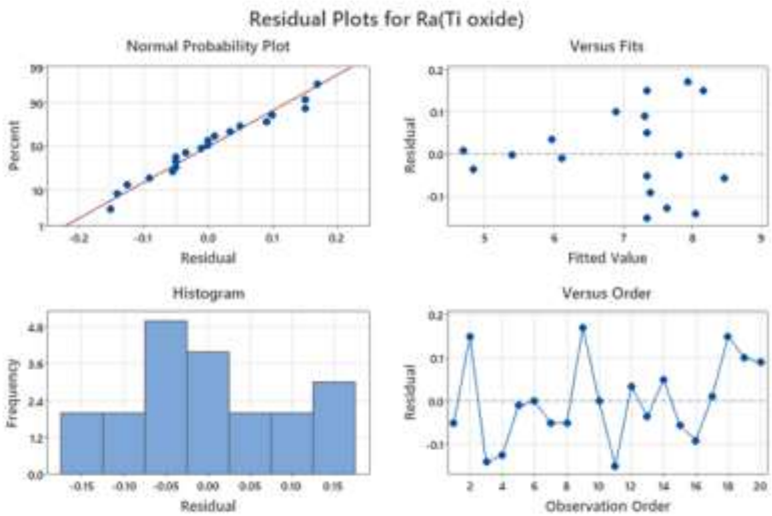

(b)

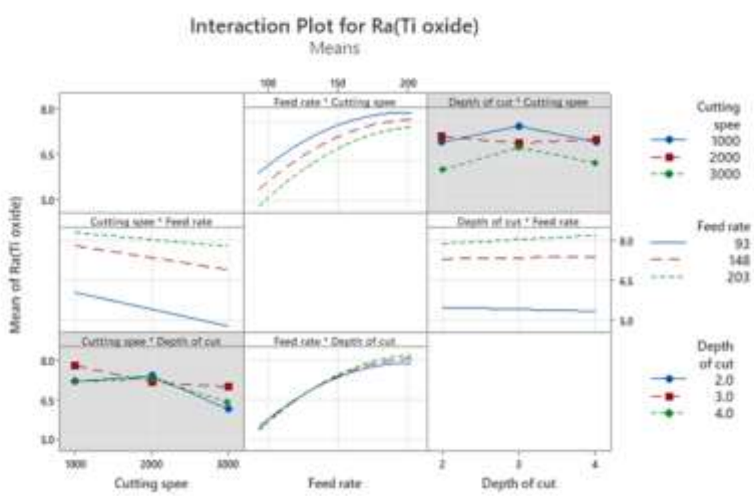

(c)

Figure 4.13: (a) Pareto plot, (b) Residual plots, and (c) Interaction plots (TiO_2)

From the main effect plot on Figure 4.13, it can be seen that the effect of feed rate on surface roughness is not linear which makes the application of response surface methodology necessary for proper identification of the effect of feed rate. From the residual plots it is seen that all the distributions are satisfactory. From the interaction plot it can be seen that there is strong interaction between cutting speed and feed rate and rather week interaction of cutting speed and depth of cut. In Figure 4.14 below, contour plot to predict R_a factor at any feed rate and cutting speed is presented.

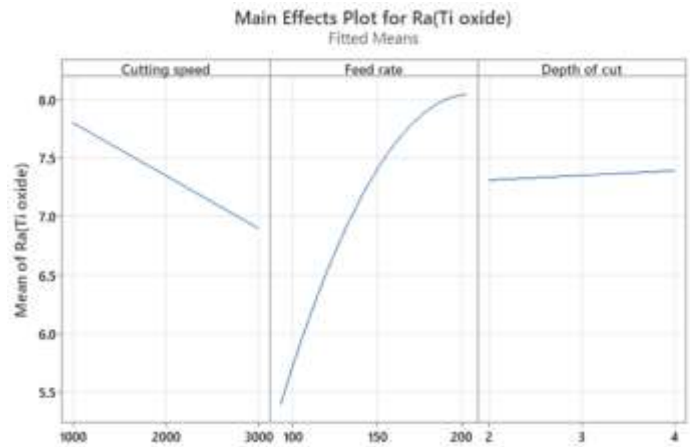

(a)

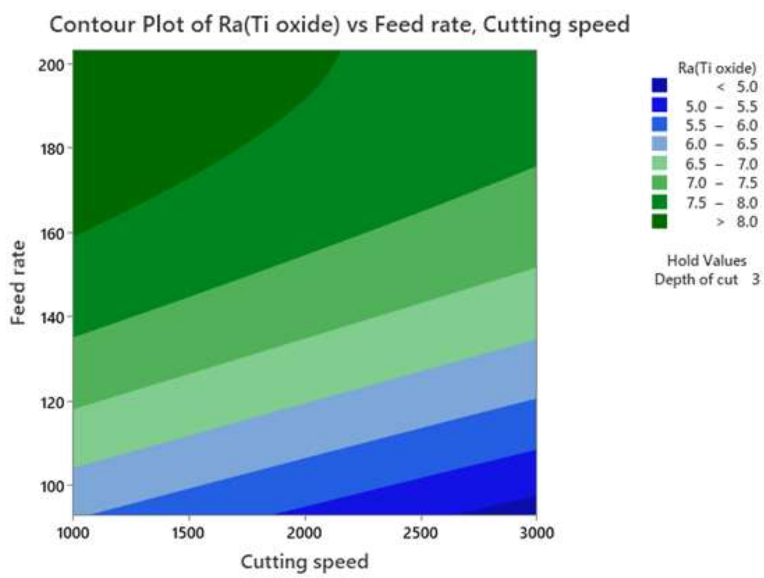

(b)

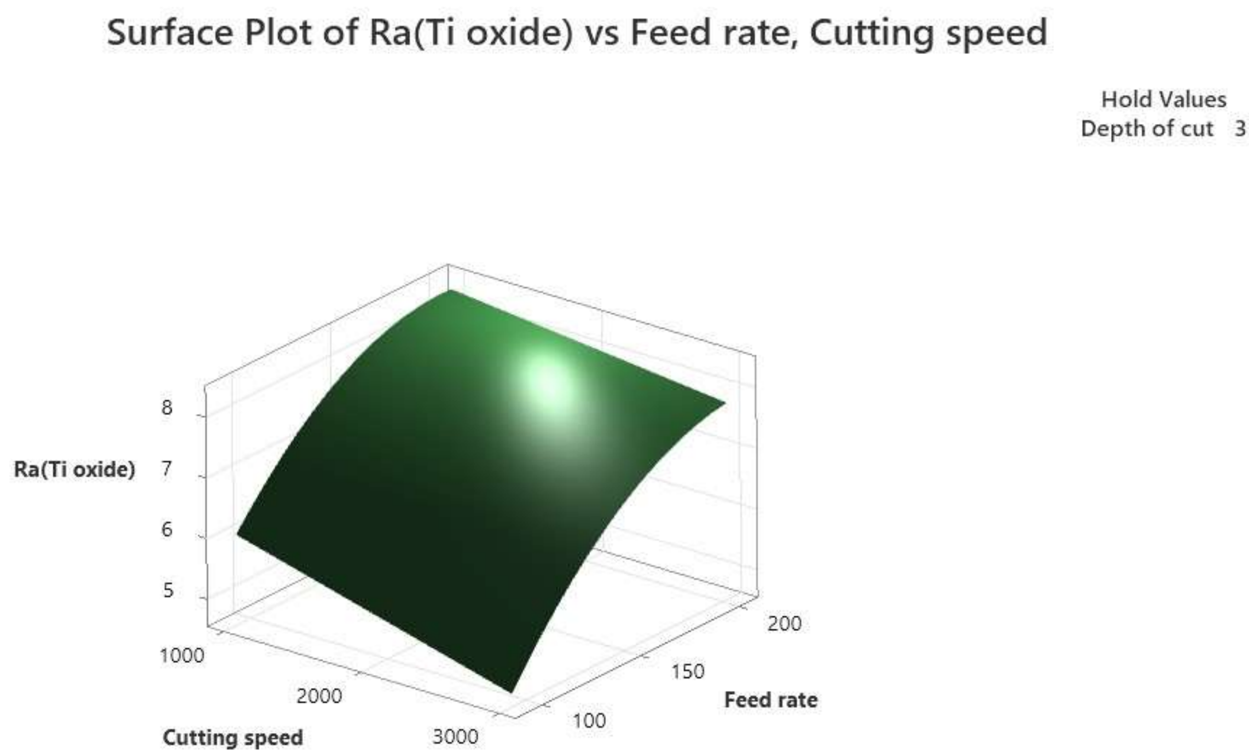

(c)

Figure 4.14: (a) Main effects plot, (b) Contour plot, and (c) Surface plot of R_a (TiO_2)

4.5.4 Optimized Response for Minimum Surface Roughness

Table 4.17: Optimized Response for R_a (TiO_2)

Parameters

Response	Goal	Lower	Target	Upper	Weight	Importance
Ra(Ti oxide)	Minimum		4.7	8.4	1	1

Solutions

Solution	Cutting speed	Feed rate	Depth of cut	Ra(Ti oxide) Fit	Composite Desirability
1	3000	93	4.00000	4.69	1
2	3000	93	3.86207	4.70	1

Multiple Response Prediction

Variable	Setting
Cutting speed	3000
Feed rate	93
Depth of cut	4

Response	Fit	SE Fit	95% CI	95% PI
Ra(Ti oxide)	4.6900	0.0931	(4.4888, 4.8912)	(4.3694, 5.0106)

Chapter 5
CONCLUSION

5.1 INTRODUCTION

In this study, natural fiber-based hybrid composite was fabricated and the machinability of the prepared samples was investigated. 3 wt.% nanofiller has been incorporated within the structure to find out the variation in the outcome. There were five layers of fiber mat in each sample whereas two of them were jute mat. Surface roughness and delamination of the samples were investigated and the analyses were conducted using Minitab2019 software. From all the machining tests, the findings are concluded below:

- Feed rate is the most significant factor which affects the most on machining factors such as delamination and surface roughness followed by cutting speed and depth of cut
- The effect of cutting speed is non-linear on delamination and the effect of feed rate on surface roughness is non-linear. This behavior persists for all the materials.
- Depth of cut has no effect on delamination or surface roughness. But in case of layered structure of composite, surface roughness can be different in different layers which resulted in some error readings in this study.
- In comparison between the three samples, composites fabricated with ZnO nanofillers provided least surface roughness factor followed by TiO_2 and Al_2O_3 .
- Among the three different samples, TiO_2 nanofiller incorporated composite provided least delamination followed by ZnO and Al_2O_3
- Comparing among the three different nanofillers it can be stated that ZnO provided the most desirable result as a nanofiller showing least overall surface roughness and moderate delamination.

5.2 FUTURE SCOPE OF STUDY

This study provides some insightful findings which can be further extended to find how different nanofillers reacts with fiber matrix bonding to enhance the properties of typical composite materials. More nanofillers can be used such as different metal oxides as well as fabricated non metal powders to find the best performance. More over woven type continuous jute fiber was used in this study which presented some difficulties during testing due to layered structure of jute and glass fiber material which can be solved by using jute and glass fiber in powder form to fabricate a homogeneous composite which will provide more accurate machinability analysis in the future. In this study tool life calculation was ignored as the main intention was to find the best possible nanofiller among the three oxides. In future, tool life can be considered as another factor to further complement the result. Also, different resin materials may have different effects on fiber matrix bonding while adding nanofillers as an enhancement method which is yet to be tested.

References

[1] S. S. R. Raj, J. E. R. Dhas, and C. P. Jesuthanam, “Challenges on machining characteristics of natural fiber-reinforced composites – A review,” *Journal of Reinforced Plastics and Composites*, vol. 40, no. 1–2, pp. 41–69, Jan. 2021, doi: 10.1177/0731684420940773.

[2] E. Taban, A. Khavanin, M. Faridan, S. E. Samaei, K. Samimi, and R. Rashidi, “Comparison of acoustic absorption characteristics of coir and date palm fibers: experimental and analytical study of green composites,” *International Journal of Environmental Science and Technology*, vol. 17, no. 1, 2020, doi: 10.1007/s13762-019-02304-8.

[3] A. K. Bledzki and J. Gassan, “Composites reinforced with cellulose based fibres,” 1999. doi: 10.1016/S0079-6700(98)00018-5.

[4] K. L. Pickering, *Properties and performance of natural-fibre composites*. 2008. doi: 10.1533/9781845694593.

[5] A. B. A. Hariharan and H. P. S. A. Khalil, “Lignocellulose-based hybrid bilayer laminate composite: Part I - Studies on tensile and impact behavior of oil palm fiber-glass fiber-reinforced epoxy resin,” *J Compos Mater*, vol. 39, no. 8, 2005, doi: 10.1177/0021998305047267.

[6] D. Wang *et al.*, “Machinability of natural-fibre-reinforced polymer composites: Conventional vs ultrasonically-assisted machining,” *Compos Part A Appl Sci Manuf*, vol. 119, pp. 188–195, Apr. 2019, doi: 10.1016/j.compositesa.2019.01.028.

[7] N. M. Nurazzi *et al.*, “A review on mechanical performance of hybrid natural fiber polymer composites for structural applications,” 2021. doi: 10.3390/polym13132170.

[8] H. Azmi, C. H. C. Haron, J. A. Ghani, M. Suhaily, and A. R. Yuzairi, “Machinability Study on Milling Kenaf Fiber Reinforced Plastic Composite Materials using Design of Experiments,” in *IOP Conference Series: Materials Science and Engineering*, Institute of Physics Publishing, Apr. 2018. doi: 10.1088/1757-899X/344/1/012027.

[9] M. M. A. Nassar, R. Arunachalam, and K. I. Alzebdeh, "Machinability of natural fiber reinforced composites: a review," *International Journal of Advanced Manufacturing Technology*, vol. 88, no. 9–12, 2017, doi: 10.1007/s00170-016-9010-9.

[10] M. K. Gupta and R. K. Srivastava, "Effect of sisal fibre loading on dynamic mechanical analysis and water absorption behaviour of jute fibre epoxy composite," in *Materials Today: Proceedings*, 2015. doi: 10.1016/j.matpr.2015.07.253.

[11] M. V. Ramana and S. Ramprasad, "Experimental Investigation on Jute/Carbon Fibre reinforced Epoxy based Hybrid Composites," in *Materials Today: Proceedings*, 2017. doi: 10.1016/j.matpr.2017.07.214.

[12] G. Seshanandan, D. Ravindran, and T. Sornakumar, "Mechanical properties of nano titanium oxide particles - hybrid jute-glass FRP composites," *Mater Today Proc*, vol. 3, no. 6, pp. 1383–1388, 2016, doi: 10.1016/j.matpr.2016.04.019.

[13] M. Hemath *et al.*, "Effect of TiC nanoparticles on accelerated weathering of coir fiber filler and basalt fabric reinforced bio/synthetic epoxy hybrid composites: Physicomechanical and thermal characteristics," *Polym Compos*, vol. 42, no. 9, pp. 4897–4910, 2021, doi: 10.1002/pc.26198.

[14] D. P. Surya, A. M. Munirah, S. S. Alamelu, J. C. H. Lau, and J. Wei, "MECHANICAL AND THERMAL PROPERTIES OF JUTE-GLASS FIBER REINFORCED NANO COMPOSITES," *IMECE2012*, pp. 1–6, 2012.

[15] L. Karthick *et al.*, "Influence of Nano- / Microfiller Addition on Mechanical and Morphological Performance of Kenaf / Glass Fibre-Reinforced Hybrid Composites," vol. 2022, 2022.

[16] N. Bharathidhasan, S. Thanigaivelan, and R. Suresh, "Sisal Fiber / Glass Fiber Hybrid Nano Composite : The Tensile and Compressive Properties Sisal Fiber / Glass Fiber Hybrid Nano Composite : The Tensile and Compressive Properties," no. December, 2014.

[17] K. Mohan and T. Rajmohan, "Effects of MWCNT on Mechanical Properties of Glass-Flax Fiber Reinforced Nano Composites," *Mater Today Proc*, vol. 5, no. 5, pp. 11628–11635, 2018, doi: 10.1016/j.matpr.2018.02.133.

[18] K. S. Raghul, M. Logesh, R. K. Kisshore, P. M. Ramanan, and G. Muralitharan, "Mechanical behaviour of sisal palm glass fiber reinforced composite with addition of nano silica," *Mater Today Proc*, no. xxxx, 2020, doi: 10.1016/j.matpr.2020.07.063.

[19] V. K. Patel, K. R. Sumesh, K. Kanthavel, and S. Vivek, "Mechanical behaviour of sisal – glass fiber reinforced hybrid Nano composites Mechanical behaviour of sisal – glass fiber reinforced hybrid Nano composites," 2018, doi: 10.1088/1757-899X/390/1/012090.

[20] M. M. Shokrieh, A. R. Kefayati, and M. Chitsazzadeh, "Fabrication and mechanical properties of clay/epoxy nanocomposite and its polymer concrete," *Mater Des*, vol. 40, 2012, doi: 10.1016/j.matdes.2012.03.008.

[21] C. I. W. Calcagno, C. M. Mariani, S. R. Teixeira, and R. S. Mauler, "The role of the MMT on the morphology and mechanical properties of the PP/PET blends," *Compos Sci Technol*, vol. 68, no. 10–11, 2008, doi: 10.1016/j.compscitech.2008.03.012.

[22] H. Y. Kordkheili, M. Farsi, and Z. Rezazadeh, "Physical, mechanical and morphological properties of polymer composites manufactured from carbon nanotubes and wood flour," *Compos B Eng*, vol. 44, no. 1, 2013, doi: 10.1016/j.compositesb.2012.04.023.

[23] M. Kishore and M. Amrita, "Mechanical characterization of jute-basalt hybrid composites with graphene as nanofiller," *Journal of Mechanical Science and Technology*, vol. 36, no. 8, 2022, doi: 10.1007/s12206-022-0714-5.

[24] J. Neto, H. Queiroz, R. Aguiar, R. Lima, D. Cavalcanti, and M. D. Banea, "A review of recent advances in hybrid natural fiber reinforced polymer composites," 2022. doi: 10.32604/jrm.2022.017434.

[25] M. Roy, *Surface engineering for enhanced performance against wear*, vol. 9783709101018. 2013. doi: 10.1007/978-3-7091-0101-8.

[26] K. Colligan and M. Ramulu, "The effect of edge trimming on composite surface plies," *American Society of MEchanical Engineers- Manufacturing review*, vol. 5, no. 4, 1992.

[27] M. Kishore, M. Amrita, and B. Kamesh, "Experimental investigation of milling on basalt-jute hybrid composites with graphene as nanofiller," in *Materials Today: Proceedings*, 2020. doi: 10.1016/j.matpr.2020.12.847.

[28] S. Al-Jawoosh, A. Ireland, and B. Su, "Fabrication and characterisation of a novel biomimetic anisotropic ceramic/polymer-infiltrated composite material," *Dental Materials*, vol. 34, no. 7, 2018, doi: 10.1016/j.dental.2018.03.008.

[29] S. Ghafarizadeh, J. F. Chatelain, and G. Lebrun, "Effect of cutting tool lead angle on machining forces and surface finish of CFRP laminates," *Science and Engineering of Composite Materials*, vol. 23, no. 5, 2016, doi: 10.1515/secm-2013-0188.

[30] M. Akmam Noor Rashid, Z. Mohd Zain, M. K. Nor Khairusshima, W. Ibne Noor, M. Mullah, and S. Ahmed Khan, "Machinability study of JFRP composite using design of experiment," *IOP Conf Ser Mater Sci Eng*, vol. 1092, no. 1, p. 012014, Mar. 2021, doi: 10.1088/1757-899x/1092/1/012014.

[31] A. Lotfi, H. Li, D. V. Dao, and G. Prusty, "Natural fiber–reinforced composites: A review on material, manufacturing, and machinability," Feb. 01, 2021, *SAGE Publications Ltd*. doi: 10.1177/0892705719844546.

[32] M. M. A. Nassar, R. Arunachalam, and K. I. Alzebdeh, "Machinability of natural fiber reinforced composites: a review," *International Journal of Advanced Manufacturing Technology*, vol. 88, no. 9–12, pp. 2985–3004, Feb. 2017, doi: 10.1007/s00170-016-9010-9.

[33] S. Vigneshwaran, M. Uthayakumar, and V. Arumugaprabu, "Review on Machinability of Fiber Reinforced Polymers: A Drilling Approach," *Silicon*, vol. 10, no. 5, pp. 2295–2305, Sep. 2018, doi: 10.1007/s12633-018-9764-9.

[34] I. M. Alarifi, "A Review on Factors Affecting Machinability and Properties of Fiber-Reinforced Polymer Composites," 2023, *Taylor and Francis Ltd*. doi: 10.1080/15440478.2022.2154304.

[35] E. Rosamah *et al.*, "The Role of Bamboo Nanoparticles in Kenaf Fiber Reinforced Unsaturated Polyester Composites," *J Renew Mater*, vol. 6, no. 1, 2018, doi: 10.7569/JRM.2017.634152.

[36] A. Mandal and D. Chakrabarty, "Studies on the mechanical, thermal, morphological and barrier properties of nanocomposites based on poly(vinyl alcohol) and nanocellulose from sugarcane bagasse," *Journal of Industrial and Engineering Chemistry*, vol. 20, no. 2, 2014, doi: 10.1016/j.jiec.2013.05.003.

[37] Y. H. Çelik, E. Kilickap, and A. İ. Kilickap, "An experimental study on milling of natural fiber (jute)- reinforced polymer composites," *J Compos Mater*, vol. 53, no. 22, 2019, doi: 10.1177/0021998319826373.

[38] G. D. Babu, K. S. Babu, and B. U. M. Gowd, "Effect of Machining Parameters on Milled Natural Fiber-Reinforced Plastic Composites," *Journal of Advanced Mechanical Engineering*, 2013, doi: 10.7726/jame.2013.1001.

[39] S. O. Ismail, H. N. Dhakal, E. Dimla, J. Beaugrand, and I. Popov, "Effects of drilling parameters and aspect ratios on delamination and surface roughness of lignocellulosic HFRP composite laminates," *J Appl Polym Sci*, vol. 133, no. 7, Feb. 2016, doi: 10.1002/app.42879.

[40] P. Chetia, S. Samanta, and T. J. Singh, "Parametric optimization in drilling of Bamboo/Basalt hybrid composite," in *Materials Today: Proceedings*, 2018. doi: 10.1016/j.matpr.2017.12.145.

[41] M. C. Murugesh and K. Sadashivappa, "INFLUENCE OF FILLER MATERIAL ON GLASS FIBER/ EPOXY COMPOSITE LAMINATES DURING DRILLING," 2012.

[42] G. H. K. Rao, M. N. M. Ansari, and S. Begum, "Effect of cutting parameters on the surface roughness of MWCNT reinforced epoxy composite using CNC end-milling process," *International Journal of Science and Research*, vol. 2, no. 11, 2013.

[43] M. Akmam Noor Rashid, Z. Mohd Zain, M. K. Nor Khairusshima, W. Ibne Noor, M. Mullah, and S. Ahmed Khan, "Machinability study of JFRP composite using design of experiment," *IOP Conf Ser Mater Sci Eng*, vol. 1092, no. 1, p. 012014, Mar. 2021, doi: 10.1088/1757-899x/1092/1/012014.

[44] A. Lotfi, H. Li, and D. V. Dao, "Machinability Analysis in Drilling Flax Fiber-Reinforced Polylactic Acid Bio-Composite Laminates," *International Journal of Materials and Metallurgical Engineering*, vol. 13, no. 9, 2019.

[45] D. Wang *et al.*, “Machinability of natural-fibre-reinforced polymer composites: Conventional vs ultrasonically-assisted machining,” *Compos Part A Appl Sci Manuf*, vol. 119, pp. 188–195, Apr. 2019, doi: 10.1016/j.compositesa.2019.01.028.

[46] F. Chegdani and M. El Mansori, “New Multiscale Approach for Machining Analysis of Natural Fiber Reinforced Bio-Composites,” *Journal of Manufacturing Science and Engineering, Transactions of the ASME*, vol. 141, no. 1, 2019, doi: 10.1115/1.4041326.

[47] S. Pujari, A. Ramakrishna, and M. S. Kumar, “Comparison of jute and banana fiber composites: A review,” *International Journal of Current Engineering and Technology,* vol. 2, no. 2, pp. 121–126, 2014.

[48] S. B. R. Devireddy and S. Biswas, “Physical and mechanical behavior of unidirectional banana/jute fiber reinforced epoxy based hybrid composites,” *Polymer composites,* vol. 38, no. 7, pp. 1396–1403, 2017.

[49] N. P. Cheremisinoff and P. N. Cheremisinoff, *Fiberglass reinforced plastics: Manufacturing techniques and applications*. William Andrew, 1995.

[50] E. Fitzer *et al.*, “Fibers, 5. Synthetic Inorganic,” *Ullmann's Encyclopedia of Industrial Chemistry*, 2000.

[51] M. Jawaid, H. P. S. A. Khalil, A. A. Bakar, and P. N. Khanam, “Chemical resistance, void content and tensile properties of oil palm/jute fibre reinforced polymer hybrid composites,” *Materials \& Design,* vol. 32, no. 2, pp. 1014–1019, 2011.

[52] E. O. Ozgul and M. H. Ozkul, “Effects of epoxy, hardener, and diluent types on the workability of epoxy mixtures,” *Construction and Building Materials,* vol. 158, pp. 369–377, 2018.

[53] C. Li, S. Qi, and D. Zhang, “Thermal degradation of environmentally friendly phenolic resin/Al2O3 hybrid composite,” *Journal of applied polymer science,* vol. 115, no. 6, pp. 3675–3679, 2010.

[54] S. Zhao, J. Zhang, S. Zhao, W. Li, and H. Li, “Effect of inorganic--organic interface adhesion on mechanical properties of Al2O3/polymer laminate composites,” *Composites science and technology,* vol. 63, no. 7, pp. 1009–1014, 2003.

[55] W.-N. Wang, I. W. Lenggoro, Y. Terashi, T. O. Kim, and K. Okuyama, "One-step synthesis of titanium oxide nanoparticles by spray pyrolysis of organic precursors," *Materials Science and Engineering: B*, vol. 123, no. 3, pp. 194–202, 2005.

[56] M. M. Kabir, H. Wang, T. Aravinthan, F. Cardona, and K.-T. Lau, "Effects of natural fibre surface on composite properties: A review," in *Proceedings of the 1st international postgraduate conference on engineering, designing and developing the built environment for sustainable wellbeing (eddBE2011)*, 2011, pp. 94–99.

[57] S. Harish, D. P. Michael, A. Bensely, D. M. Lal, and A. Rajadurai, "Mechanical property evaluation of natural fiber coir composite," *Materials characterization*, vol. 60, no. 1, pp. 44–49, 2009.

[58] M. M. Kabir, H. Wang, K. T. Lau, and F. Cardona, "Chemical treatments on plant-based natural fibre reinforced polymer composites: An overview," *Composites Part B: Engineering*, vol. 43, no. 7, pp. 2883–2892, 2012.